

Copy 60

NASA Project Apollo Working Paper No. 1061

PROJECT APOLLO

EVALUATION OF ABLATION HEAT SHIELD MATERIAL SPECIMENS

INCORPORATING ELECTRICAL CONNECTORS

PHASE I

FACILITY FORM 602

N 70-34432

(ACCESSION NUMBER)

42

(THRU)

TMX-64299

(PAGES)

(CODE)

09

(CATEGORY)



NATIONAL AERONAUTICS AND SPACE ADMINISTRATION

MANNED SPACECRAFT CENTER

Houston, Texas

November 26, 1962

NASA PROJECT APOLLO WORKING PAPER NO. 1061

PROJECT APOLLO

EVALUATION OF ABLATION HEAT SHIELD MATERIAL SPECIMENS

INCORPORATING ELECTRICAL CONNECTORS

PHASE I

R. T. Gundersen

R. T. Gundersen
Project Engineer

Authorized for Distribution:

Maxime A. Faget

Maxime A. Faget
Assistant Director for
Research and Development

NATIONAL AERONAUTICS AND SPACE ADMINISTRATION

MANNED SPACECRAFT CENTER

Houston, Texas

November 26, 1962

TABLE OF CONTENTS

Section	Page
SUMMARY	1
INTRODUCTION	1
SYMBOLS	2
TEST OBJECTIVES	2
TEST DESCRIPTION	3
MATERIAL AND SPECIMEN DESCRIPTION	4
RESULTS AND ANALYSIS	5
Observation and Evaluation	5
Temperature and Weight Measurement	6
Specimen Test Results	7
CONCLUDING REMARKS	8
REFERENCES	8
TABLE I	9
TABLE II	10
FIGURES 1 to 28	11 to 38

LIST OF FIGURES

Figure	Page
1 Electrical Interface Connector	11
2 Electrical Contact Details	12
3 Photograph of the 2500-Kilowatt Arc Jet Facility	13
4 Pictorial View Showing Configuration of 2500-Kilowatt Arc Jet	14
5 Details of Specimen, Mounting, and Instrumentation . .	15
6 Electrical Interface Specimen	16
7 Insert Arrangement 240-Second Test Specimen	17
8 Typical Time History of Surface Temperature (240-Second Test Shown) Material - Phenolic-Nylon W/Microballoons .	18
9 Insert Arrangement (Random Hole Patterns) 200-Second Test Specimen	19
10 Profile Photograph of 200-Second Specimen (Before Test).	20
11 Profile View Showing Appearance After 200-Second Test .	21
12 Insert Arrangement - 160 - and 80-Second Test Specimen .	22
13 Contour and Hole Depth Measurements (80-Second Test). .	23
14 Contour and Hole Depth Measurements (160-Second Test) .	24
15 Contour and Hole Depth Measurements (240-Second Test) .	25
16 Temperature - Time History (Test Exposure Time - 80-Second)	26
17 Temperature - Time History (Test Exposure Time - 160-Second)	27
18 Temperature - Time History (Test Exposure Time - 240-Second)	28

LIST OF FIGURES

Figure	Page
19 Temperature - Time History for Socket Contacts (Test Exposure Time - 240-Second)	29
20 Time History of Surface Recessi and Char Growth	30
21 Comparison of Weight Loss	31
22 Comparative Ablation of Phenolic-Nylon W/Microballons Specimen	32
23 Top View of Model 2 Showing Effect of 240-Second Exposure to the Test Environment	33
24 Profile View of Model 3 Showing Effect of 240-Second Exposure to the Test Environment	34
25 Top View of Model 4 Showing Effect of 160-Second Exposure to the Test Environment	35
26 Profile View of Model 4 Showing Effect of 160-Second Exposure to the Test Jet Environment	36
27 Top View of Model 6 After 80 Seconds Exposure to the Test Environment	37
28 Profile View of Model 6 After 80 Seconds Exposure to the Environment	38

EVALUATION OF ABLATION HEAT SHIELD MATERIAL SPECIMENS

INCORPORATING ELECTRICAL CONNECTORS

PHASE I

SUMMARY

A preliminary study was made of the feasibility of passing an electrical conductor through the heat shield of the Apollo Command Module. The study included tests of seven specimens of phenolic-nylon material in the Langley Research Center 2500-KW Arc-Jet in the High Temperature Materials Laboratory. The three-inch diameter specimens contained patterns of holes of various diameters and depths. The data indicate that the holes had negligible effect on the integrity and ablation characteristics of the heat shield. The results indicate the feasibility of this design approach to provide electrical interface connections through ablative materials.

INTRODUCTION

One of the major problems in spacecraft is the location and design of the electrical interface between modules of the spacecraft. The Apollo configuration has an electrical interface problem of considerable magnitude between the command module and service module. It is estimated that the total number of electrical wires between the two modules ranges between 600 and 800. Most of these wires require number 16 or number 20 wire connectors.

The Mercury capsule utilized five umbilicals with a 144-wire capacity. In addition, the Mercury capsule ground test umbilical had a capacity of 106 wires. Thus, the Apollo spacecraft with 600 to 800 wire leads would require seven umbilical plugs similar to the Mercury ground test umbilical. Obviously the electrical interface problem for Apollo is considerably greater than that for Mercury.

A test program was undertaken to investigate the feasibility of providing electrical connection between the Apollo Command and Service Modules by means of a multi-conductor cable with a separable pin-and-socket connector in the ablation heat shield of the command module. The technique consists of embedding the socket elements of the connector at some depth in the heat shield material and providing sufficiently long pins on the mating parts of the connector for proper electrical contact.

It is recognized that the proposed electrical interface must be designed to survive a severe flight environment. Reentry upon return from lunar missions will be characterized by short-duration heating at very high heat transfer rates, and long duration heating at lower heating rates. The high heating rates exceed $500 \text{ BTU}/\text{ft}^2\text{-sec}$ for 200 seconds duration and the low rates of below $50 \text{ BTU}/\text{ft}^2\text{-sec}$ are encountered for times approaching 1,000 seconds. Large areas of the Apollo vehicle may have maximum radiation equilibrium temperatures greater than 4000°F .

The test program was successfully completed on April 27, 1962 in the Langley Research Center (LRC) 2500-KW Arc Jet at the High Temperature Materials Laboratory. Valuable help was received from Andrew J. Chapman III, Structures Research Division, Entry Structures Branch in the role of Project Engineer for LRC.

SYMBOLS

TC	Thermocouple
T_s	surface temperature, $^{\circ}\text{F}$
q	average heating rate, $\text{BTU}/\text{ft}^2\text{-sec}$
T	temperature, $^{\circ}\text{F}$
t	time from insertion of specimen into arc jet, sec
R	model radius, inches
CL-AL	No. 30 chromel-alumel
D	diameter, inches
C_v	visual char depth, inches

TEST OBJECTIVES

The purpose of this test program is to investigate the effect of holes for the electrical interface on the integrity and ablation characteristics of a charring heat shield material. Specifically, the test program investigates the feasibility of providing electrical connection between the Apollo Command and Service Modules utilizing a

multiconductor cable with a separable pin-and-socket connector at the ablation heat shield of the command module, as shown in figure 1. Figure 2 illustrates the technique of embedding the socket elements of the connector at some depth in the heat shield material and providing sufficiently long pins on the mating part of the connector for electrical contact. Thus, during reentry the heat shield would present a surface containing many small holes at the location where the connector was disconnected.

The following measurements and analyses were made to evaluate the behavior of the ablation material:

1. Temperature at each pin hole depth level and in the 3-socket contact solder pots
2. Hole depth and contour
3. Surface temperature
4. Stream temperature and stagnation temperature
5. Visual examination of sectioned specimen
6. Weight loss
7. Motion analysis of color motion pictures of tests

TEST DESCRIPTION

The investigations were carried out in an electric arc-powered air jet using the experimental arrangement shown in figure 3. Figure 4 is a pictorial view showing the details of the 2500-kilowatt 3-phase A-C arc jet. Electric arcs are drawn between water-cooled copper ring electrodes. Each pair of ring electrodes is energized by one phase of the three-phase power supply. The arcs drawn between the concentric ring electrodes are rotated by a magnetic field created by the coils surrounding the arc chamber. Air is admitted to the chamber below the arcs, passes through the arcs, and is heated to temperatures up to about 9000°F, depending on the power input and air flow. This heated air is directed onto the specimens by the nozzle at the top of the arc chamber. The test specimens were supported on a water-cooled sting. See reference 1 for a more detailed facility description.

The tests were conducted by placing the test specimen one inch from the jet nozzle with its surface perpendicular to the jet stream.

Heating rates of 110 BTU/ft²-sec for periods of 240, 200, 160, and 80 seconds and a maximum surface temperature of 3520°F were attained. Figure 5 shows details of specimen, mounting and instrumentation. Table 1 describes the test program in terms of test duration, total heat pulse, and visual char depth.

Hole depth and contour measurements from the front surface were taken before and after each test utilizing a precision depth gauge. For surface temperature measurement a Leeds and Northrup optical pyrometer was employed. Thermocouple temperatures were recorded by oscilloscope. A spectrograph was utilized for measurement of stream temperatures. A motion analyzer was used for analysis of the color motion pictures of the tests. After the specimens received a protective epoxy coating, the specimens were precision-sectioned and sanded to permit visual examination of the material and connectors.

MATERIAL AND SPECIMEN DESCRIPTION

The test material of model 1 consisted of an equal-weight mixture of phenolic resin and powdered nylon without microballoons as a reference material. The material for models 2 through 7 was a mixture of equal weights of phenolic resin and nylon with 50-percent of the phenolic in the form of microballoons. This material represents one of the best thermal protection materials available and was compounded by the Materials Processing and Development Section of Langley Research Center.

This material is somewhat similar to the proposed Apollo heat shield material, namely AVCOAT 5026, which has an epoxy resin base. The test specimen material has the following characteristics:

1. Develops good char.
2. Ablates at high surface temperature.
3. Chemical reactions produced by-products which both absorb and block incoming heat
4. Has relatively low density, 36 lbs/ft³.

Each three-inch diameter instrumented specimen was initially 1.75 inches thick and contained chromel-alumel thermocouples embedded at varying depths from the front face as shown in figures 6 and 7. These figures show the initial hole pattern with the minimum allowable spacing required for a prototype connector. Figure 6 illustrates the hole depths, thermocouple installation technique, and socket contact installation.

Model 2 also had CL-AL thermocouples embedded in the solder well of the socket contacts at three different depths. It was deemed necessary to test a blank specimen prior to the hole pattern specimen to serve as a reference for determining the affect of the holes on ablation behavior. The blank specimen also served to determine the maximum allowable test time for the instrumented specimens.

RESULTS AND ANALYSIS

Observation and Evaluation

High surface temperatures, which are possible when chars are present, result in increased thermal protection efficiency because large amounts of heat are lost by re-radiation. However, heat conduction into the material is strongly influenced by the surface temperature. In the tests of this program, front surface temperatures of the specimens were measured with an optical pyrometer and are presented in table II and figure 8.

A preliminary test of 200 seconds duration was conducted on Model 1 (see figure 9) which has a phenolic-nylon material without microballoons. Figure 9 shows the random hole pattern for No. 16 and 20 pins with copper wire backing to simulate socket contacts. Hole depths were established in .25-inch increments to 1.00-inch total depth. This test specimen was placed one inch from the jet nozzle with its surface perpendicular to the jet stream and subjected to a heating rate of 100 BTU/ ft^2 -sec for a period of 200 seconds. The surface temperature was 3500°F and the stream temperature was 6920°F. The visual char depth was .25 inches. Early test results indicated no general breakdown of the char material in the regions of the hole clusters. There was a moderate increase of total surface regression at hole cluster locations and a tendency for holes to fill with eroded material. Figure 10 shows the smooth contour of the 200-second specimen before exposure. Figure 11 shows some of the results of 200 seconds exposure to the arc-heated air stream, including the severe side erosion caused by the characteristic airflow over the side of the model.

Figures 7 and 12 illustrate the insert arrangements for the 240-, 160-, and 80-second tests. Figures 13, 14 and 15 present scaled drawings of sectioned specimens which show the development of char on the phenolic-nylon composition at a convective heating rate of 110 BTU/ ft^2 -sec. Figure 13 (80-second test) shows no effect of the heating on hole depths; even the shallowest holes, .344-inch deep, showed no change in depth. Figure 14 (160-second test) shows a more advanced state of ablation with the .344-inch depth holes completely removed. Holes with depths of .688-inch, or

more, were filled partially with eroded material. Figure 15 indicates that all of the material containing holes has been ablated after a test of 240 seconds duration.

For 80-second exposures, the surface temperature was about 3500°F and very slight change in size and shape occurred. A moderate layer of char was formed over the surface of the specimen. As the test time increased to 160 seconds, the temperature peaked at 3500°F and remained essentially constant thereafter. The char thickness increased and moderate changes occurred in shape and size. In tests of 240 seconds duration the size and shape of the specimen changed greatly. The severe erosion on the sides of the specimens result from the characteristics of the airflow about the specimens.

It should be noted that char removal and the associated mass loss are greatly influenced by the oxygen content of the test stream. In a high-altitude flight environment, where there is less oxygen, weight loss could be less than under sea level conditions. When analyzing experimental results, problems also arise because of uncertainty in material properties, such as char conductivity, specific heat of the gases resulting from pyrolysis, heat and temperature of pyrolysis.

Temperature and Weight Measurement

Temperature is plotted as a function of time for several stations measured from the front surface and thermocouple readings are presented in figures 16 through 19 for all instrumented tests. Figure 16 (80-second test) shows that TC-5, located at a depth of .74 inches from the front surface of the model, had a very rapid temperature rise and reached its peak temperature of 1509°F at 83-second exposure time. All other thermocouples peaked at later times and at much lower temperatures, after the removal of the model from the arc stream. The maximum temperature rise of TC-5 was probably influenced by the erosion of specimen sides and edge failure in the severe arc jet environment. TC-1 and TC-5 are at the same depth level, but TC-1 is better protected by its more central location and peaked at 160°F during the cooling cycle. TC-6 peaked at 300°F before being burned out with a resulting thermocouple failure. The omission of TC-4 is due to thermocouple failure.

Figure 17 (160-second test) again shows that TC-5 located at a depth of .74 inches from the front surface had a rapid temperature rise and reached its peak temperature of 2124°F at the cessation of the heating pulse. After the removal of the model from the arc stream, TC-2 peaked at 1457°F at 320 second exposure time, during the cooling cycle. TC-1 and TC-3 peaked at much later times and much lower temperatures. The omission of TC-4 is the result of thermocouple failure.

Figure 18 (240-second test) shows that TC-6, located closest to the front surface of the model, had a very rapid temperature rise and reached its peak temperature of 2340°F at 125 seconds exposure time when it experienced burn-out. TC-8 and TC-9 again show the high temperature effect of severe side erosion and the subsequent burn-out effect. The TC-4 measured junction of .56 inches depth peaked at 1708°F at 155 second exposure time of burn-out. The TC-7 measured junction of .74-inch depth peaked at 1067°F at 200 second exposure time. The low recording of TC-5 is due to a faulty thermocouple.

Figure 19 shows the temperature-time history of the socket contacts with an exposure time of 240 seconds. TC-3, located closest to the front surface of the model had a temperature rise of 946°F at the cessation of the heating pulse. TC-1 and TC-2 temperatures were comparably lower for interior thermocouple junctions.

Figure 20 shows the regression with time of the front face and char-virgin material interface of the specimen. The front face receded slowly at first but the rate of recession increased with time.

Comparison of weight loss is presented in Figure 21. Weight loss in grams is plotted as a function of time for the blank specimen and for the hole pattern specimen.

Figure 22 indicates the comparative ablation of the 160 and 240-second test specimens by comparing these models with their respective blank reference model. The 80-second test differential was too slight for comparison. For documentation purposes, figures 23 and 24 show the after effects of the 240-second test. Figures 25 and 26 show the appearance of a model after the 160-second test. Figures 27 and 28 show the appearance of a model after the 80-second test.

Specimen Test Results

Visual inspection of sectioned specimens and measurements of contour and hole depth were made. As previously stated, figures 15, 16, and 17 illustrate the test effects on the comparative models. Thus, it should be noted that the following test results were obtained:

1. A small difference in weight loss between a blank specimen and a hole specimen for the same test times.
2. A tendency for pin holes to fill up with eroded material.
3. Blank specimen had smooth contours, whereas specimens with holes showed a slight cratering at the entrances to the holes.

4. No general breakdown of the char layer in the region of the hole cluster.
5. Slight increase of total surface recession at hole cluster locations.
6. No significant increase of char layer thickness in hole cluster region relative to char layer thickness in blank specimens.
7. Pin holes tend to seal with eroded material.

CONCLUDING REMARKS

The limited test program indicated that the addition of pin holes and socket contacts had negligible effect on the integrity and ablation characteristics of the heat shield material. It is recommended that in view of these results an extension of the program is warranted, for specimens of the actual Apollo materials, using existing ground testing apparatus and eventually testing a prototype electrical interface in a flight environment.

REFERENCES

1. Kotanchik, Joseph N., and Ross, Robert D.: Electric Arc-Powered Research Facilities for Materials and Structures Testing, NASA, LRC, Presented to the Annual Winter Meeting of ASME, New York, N. Y., Nov. 26-Dec. 1, 1961.
2. Geogiev, S.: Hypersonic Ablation and Interpretation of Test Results, AVCO-Everett Research Laboratory Res. Report 99, October 1960.
3. Swann, Robert T.: A Theoretical Study of Ablation Shield Requirements for Manned Reentry Vehicles, NASA, LRC N-51086, 1960.
4. Brooks, William A., Jr., Wadlin, Kenneth L., and Swann, Robert T.: Thermal Protection for Spacecraft Entering at Escape Velocity, NASA, LRC, Presented to the National Aeronautics Meeting of SAE, New York, N. Y. April 3-6, 1962.
5. Kotanchik, Joseph N., and Wadlin, Kenneth L.: The Use of Ablators for Achieving Protection Against High Thermal Flux, NASA, LRC, Presented to the 1961 SAE Aerospace Engr. & Mfg. Meeting, Los Angeles, Calif. Oct. 9-13, 1961.

TABLE I
Test Program of Ablation Heat Shield Material Specimen
Incorporating Electrical Connectors

(Heating Rate - 110 Btu/ft²-sec)

Model Number	Type	Test Duration t, Seconds	Total Heat Pulse (Btu/ft ² -sec)	Visual Char Depth, Inches
1	LRC-Random Hole Pattern	200	22,000	.250
2	MSC Specimen-Hole Pattern	240	26,400	.156
3	MSC Blank	240	26,400	.156
4	MSC Specimen-Hole Pattern	160	17,600	.156
5	MSC Blank	160	17,600	.188
6	MSC Specimen-Hole Pattern	80	8,800	.156
7	MSC Blank	80	8,800	.188

TABLE II
SURFACE TEMPERATURE TEST DATA

Time, Seconds	Surface Temperature °F				80 sec (Blank)
	240 sec (W/Blank)	240 sec (Blank)	160 sec (W/Holes)	160 sec (Blank)	
10	3000		3100		3200
15			3410		3310
20			3210		3520
35			3280		3440
40	3450		3480		
45		3370			
55		3480			
60		3460			
62		3470			
80	3500		3500		
85		3470			
110	3520		3500		
115			3450		
125			3460		
145		3500			
170		3450			
205		3500			
230		3520			

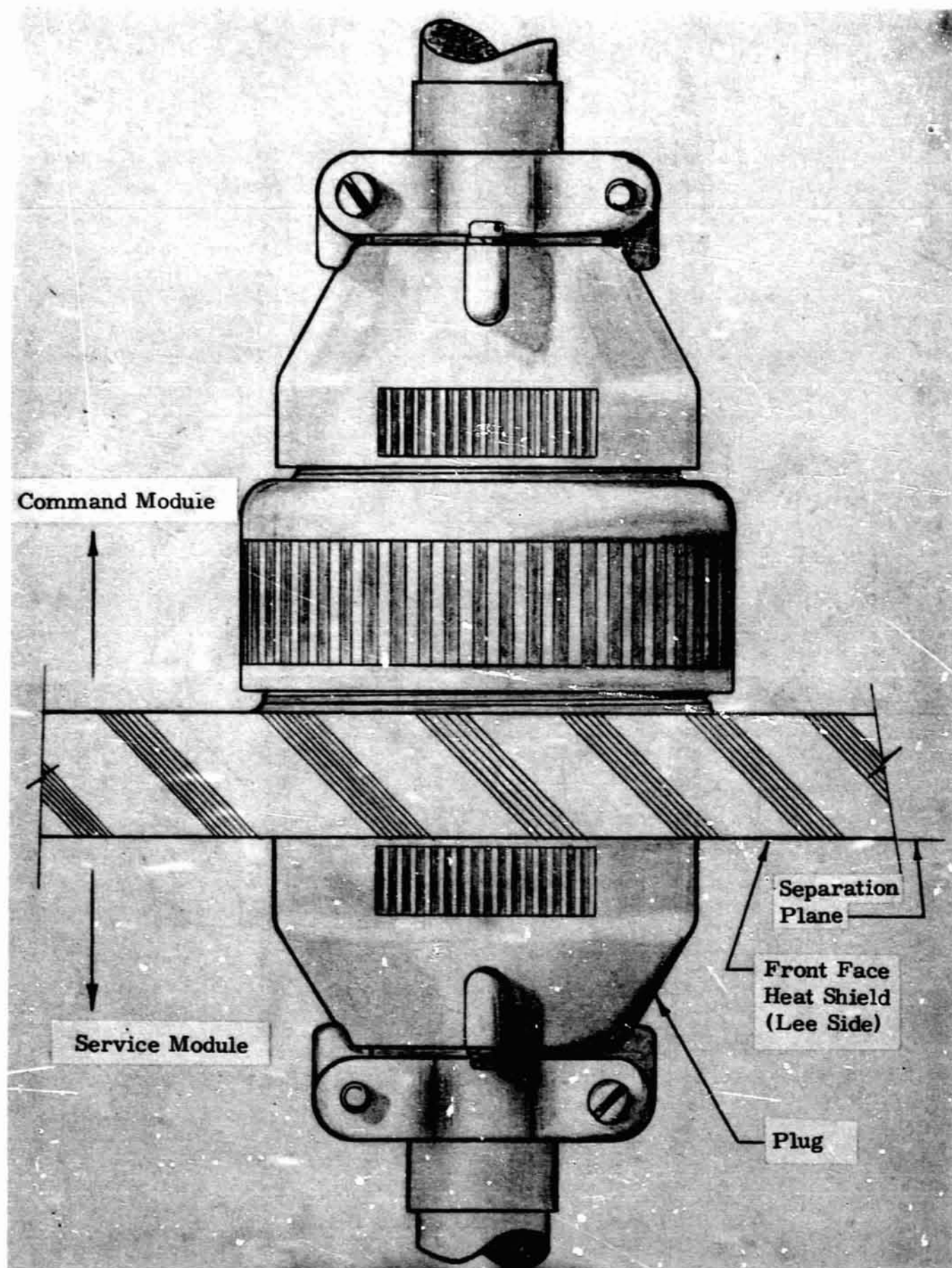


Figure 1 - Electrical Interface Connector

12

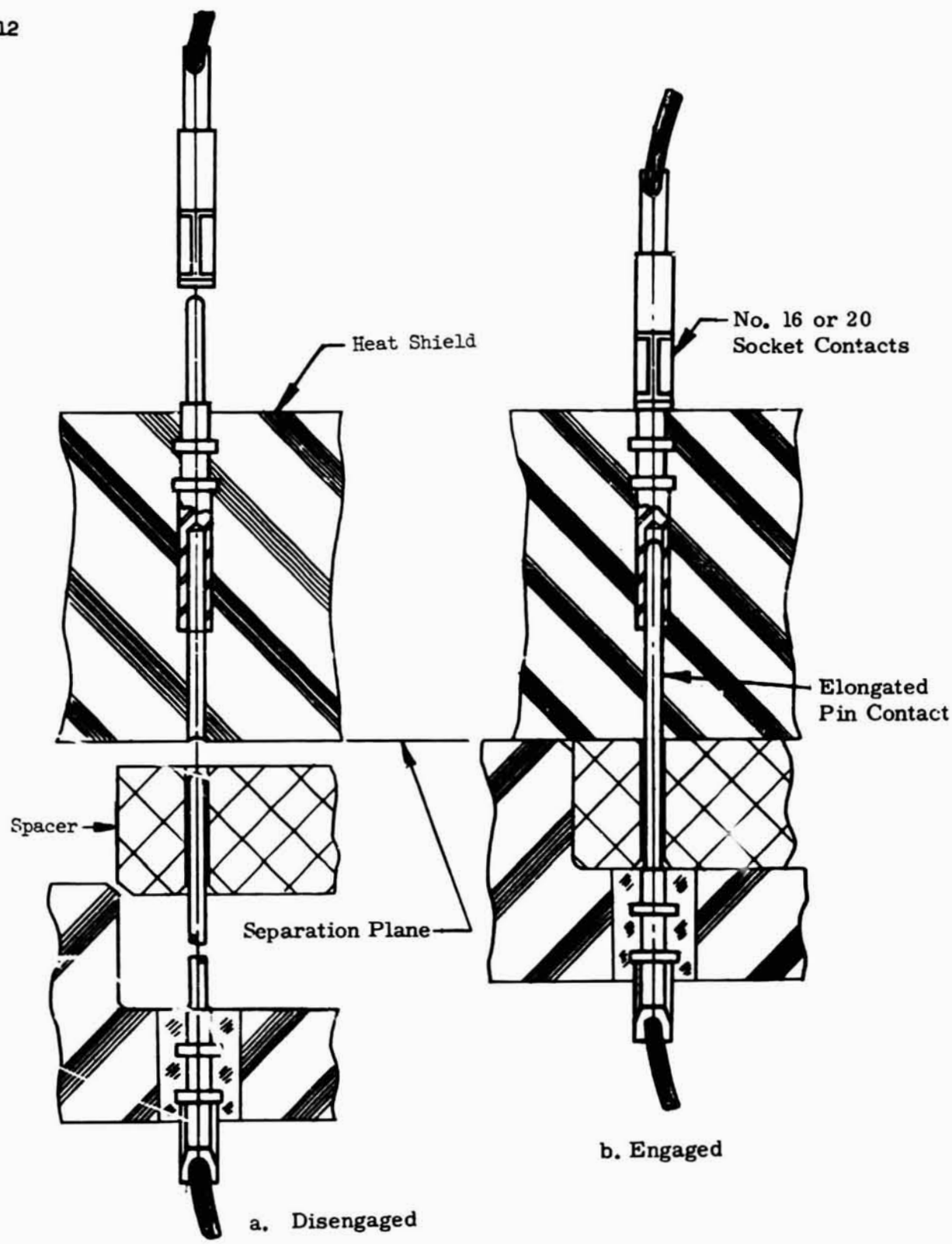


Figure 2 - Electrical Contact Details

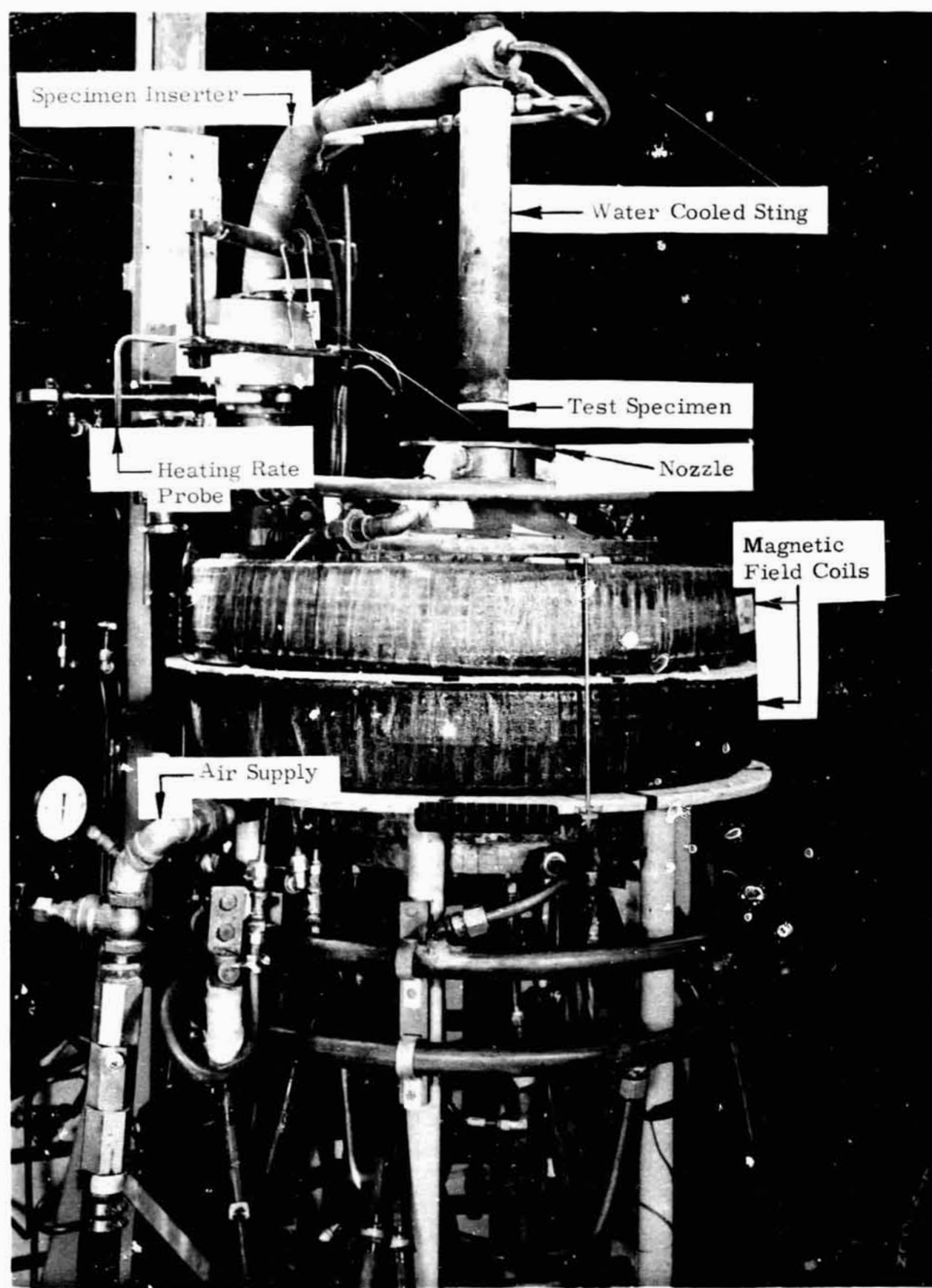


Figure 3 - Photograph of the 2500-Kilowatt Arc Jet Facility

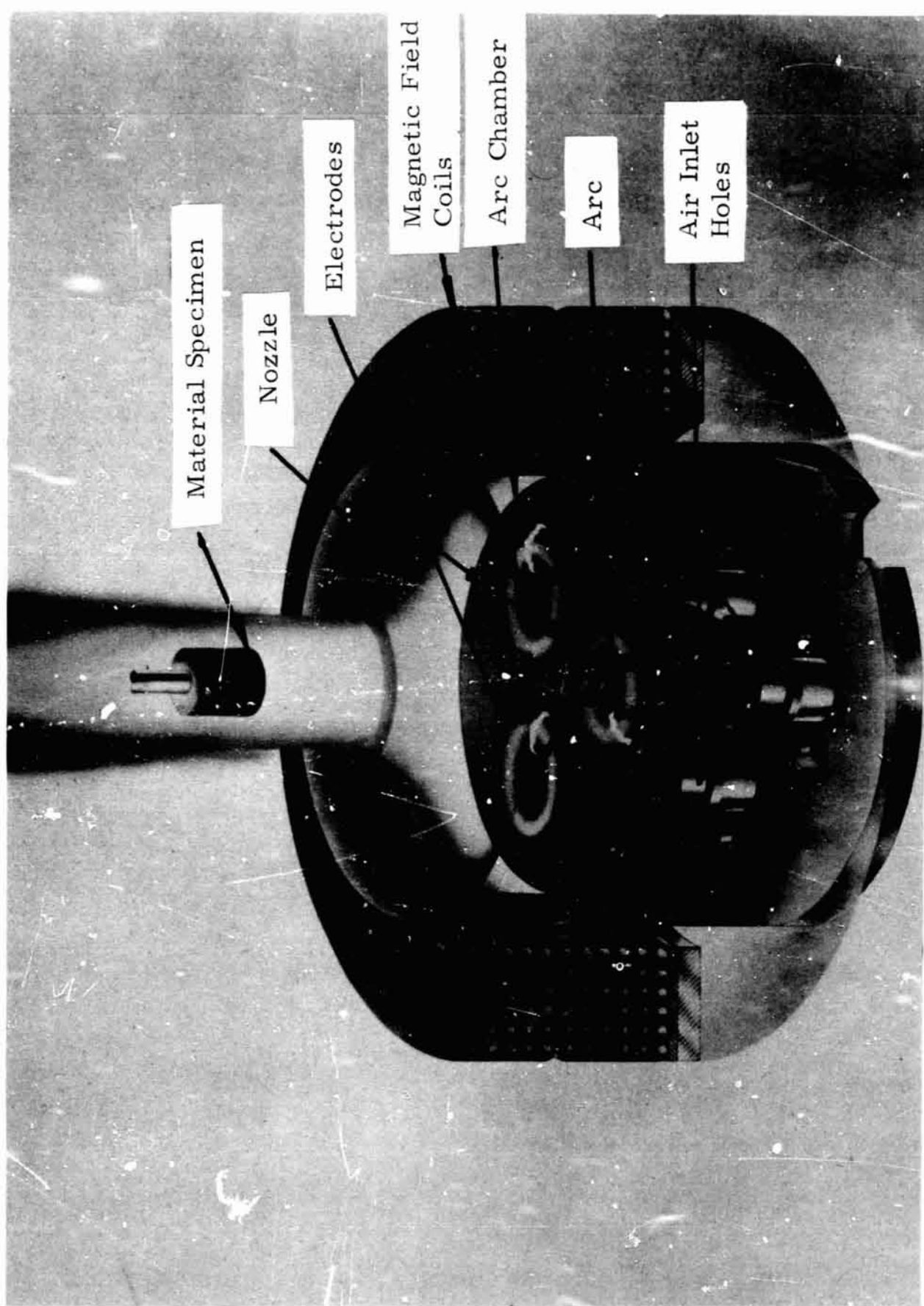


Figure 4 - Pictorial View Showing Configuration of 2500-Kilowatt Arc Jet

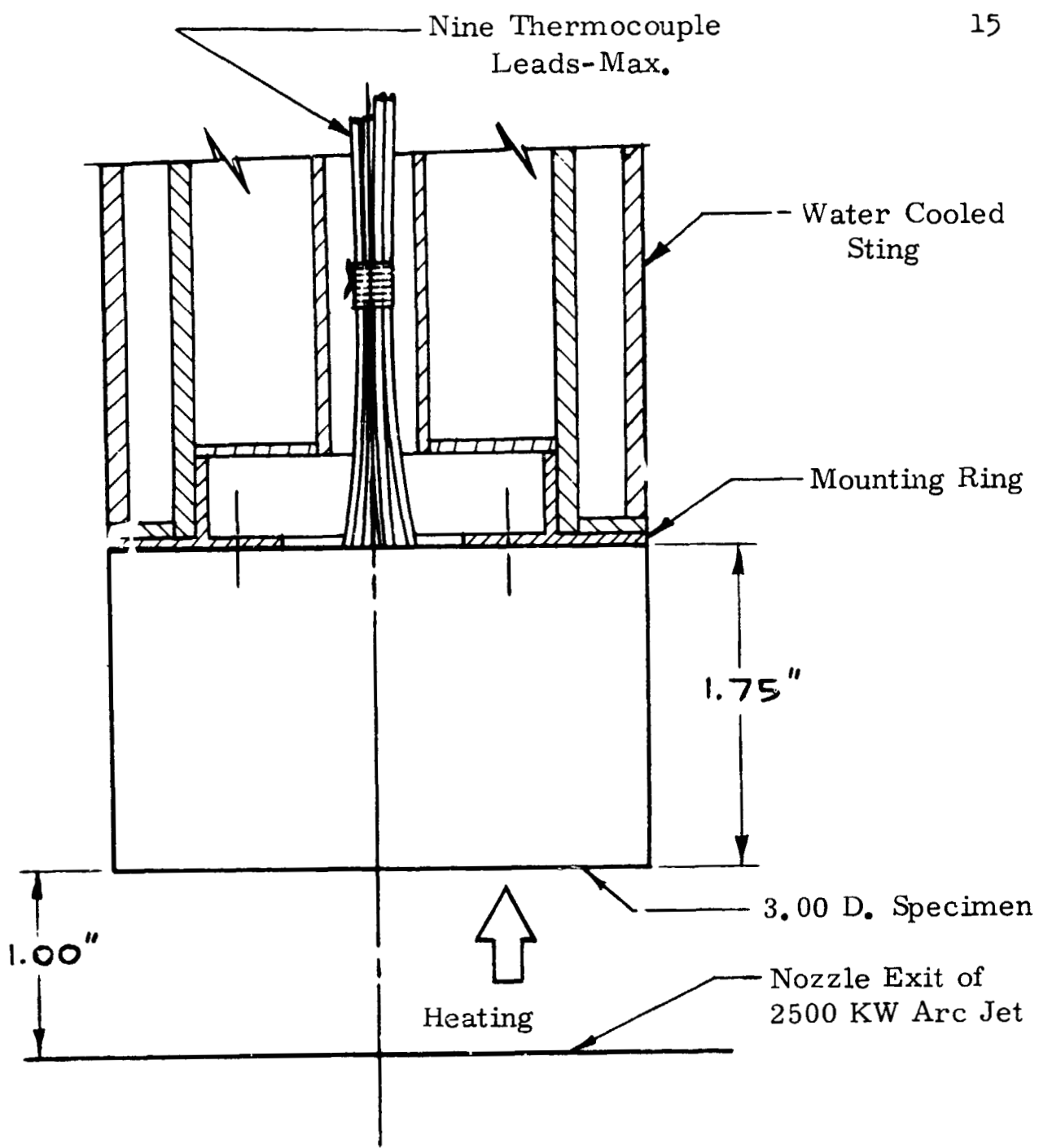


Figure 5 - Details of Specimen, Mounting, and Instrumentation

16

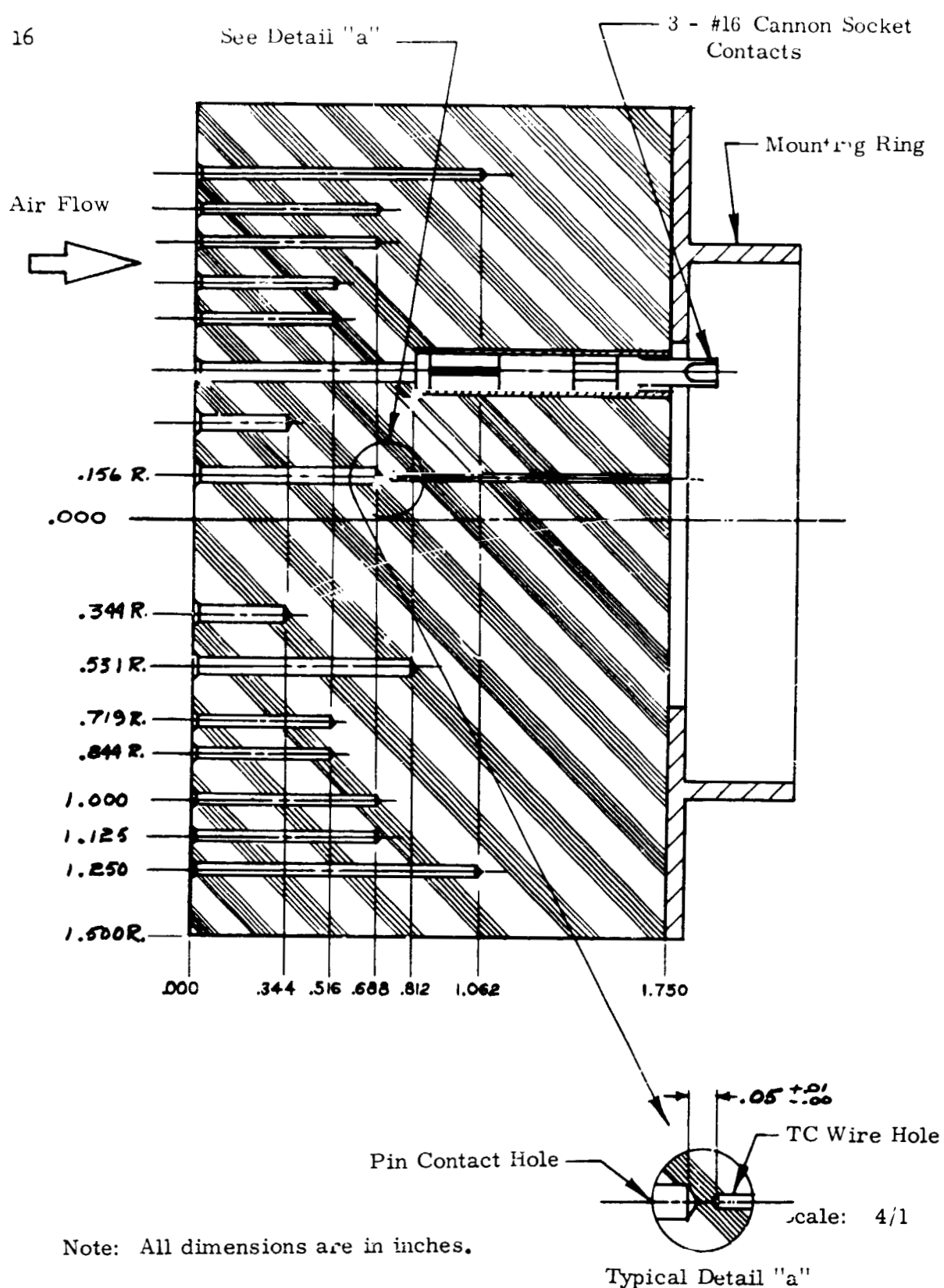
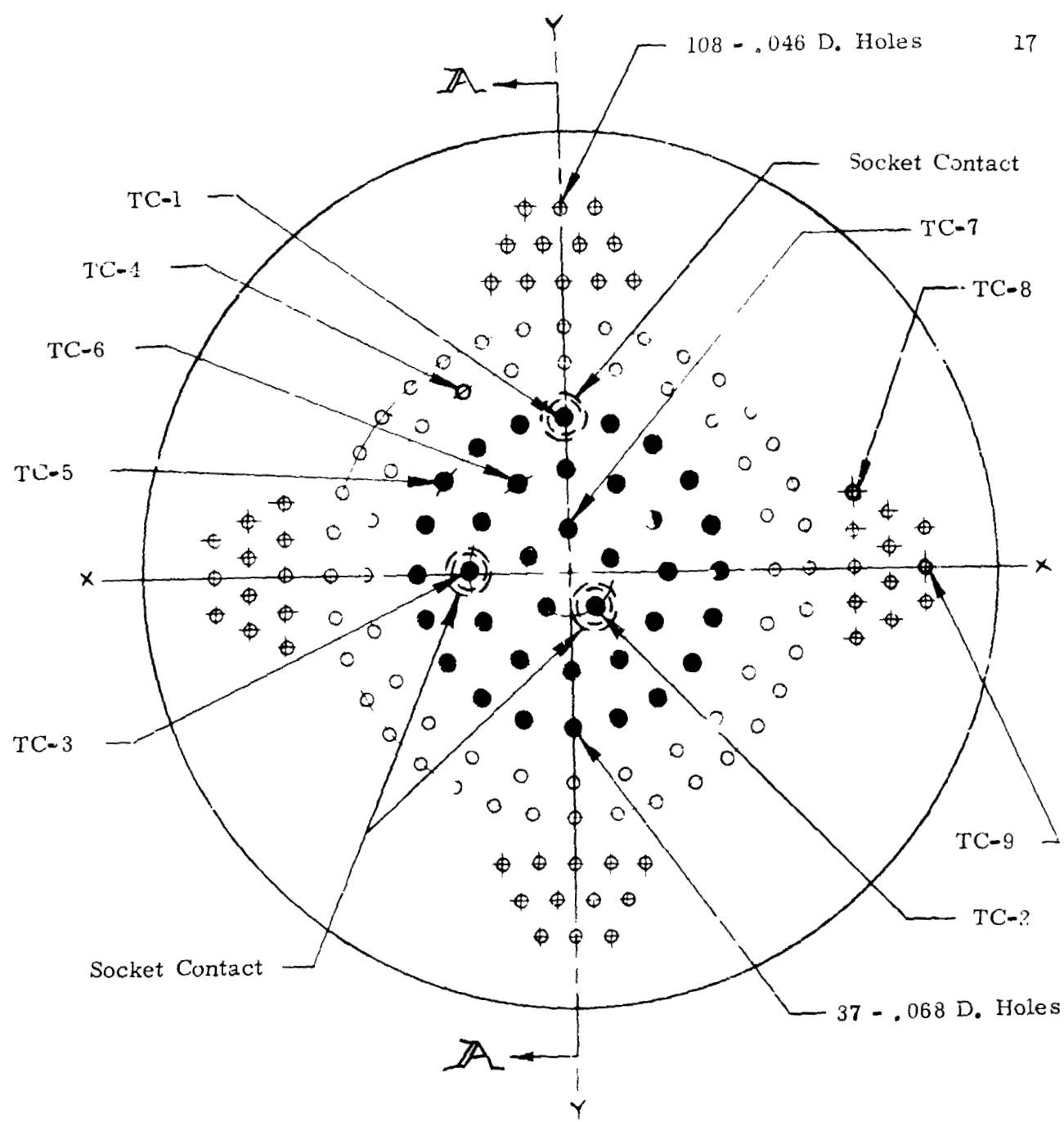


Figure 6 - Electrical Interface Specimen



LEGEND:

- - No. 16 Pin Hole (For No. 16 and 14 Ga. Wire Leads)
- - No. 20 Pin Hole (For No. 18, 20, and 22 Ga. Wire Leads)
- TC - Thermocouple Locations

Figure 7 - Insert Arrangement
240-Second Test Specimen

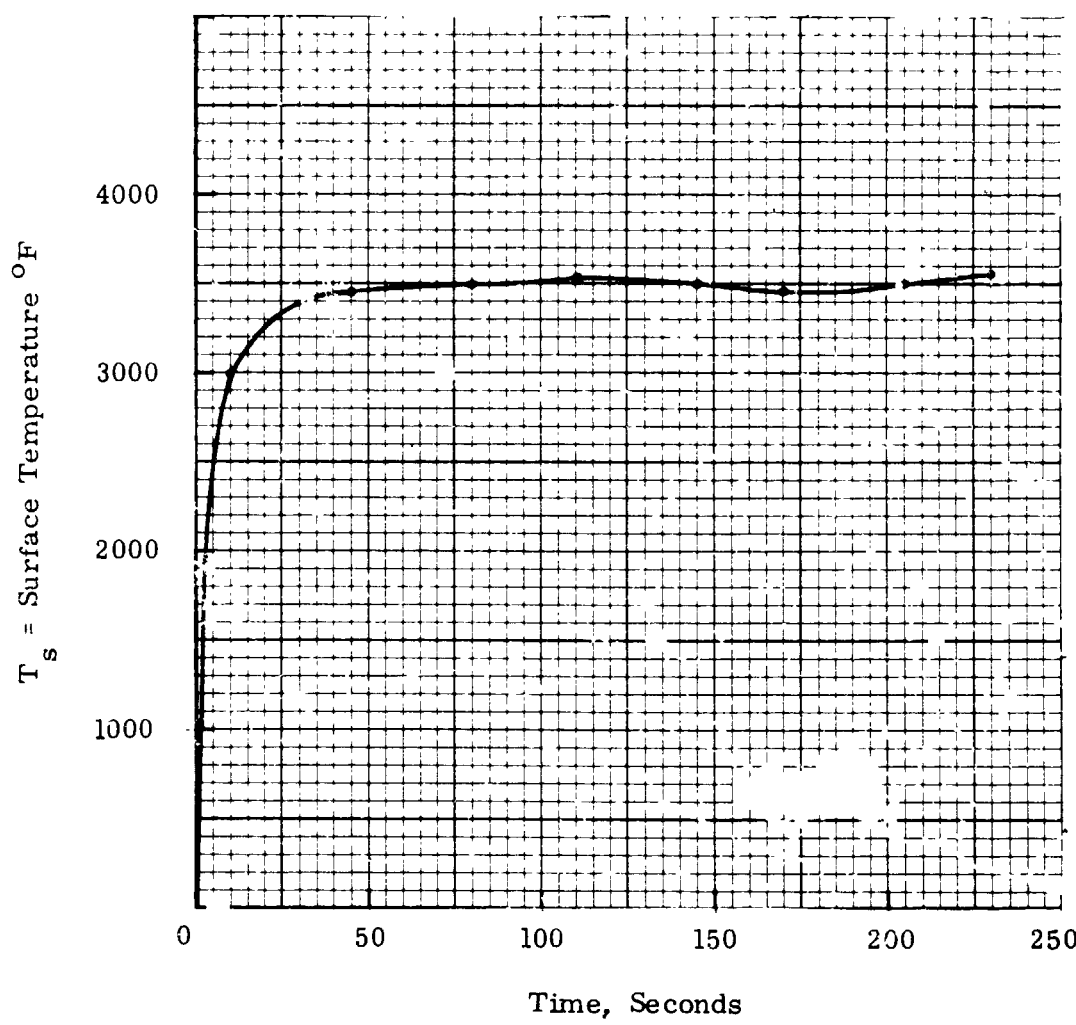
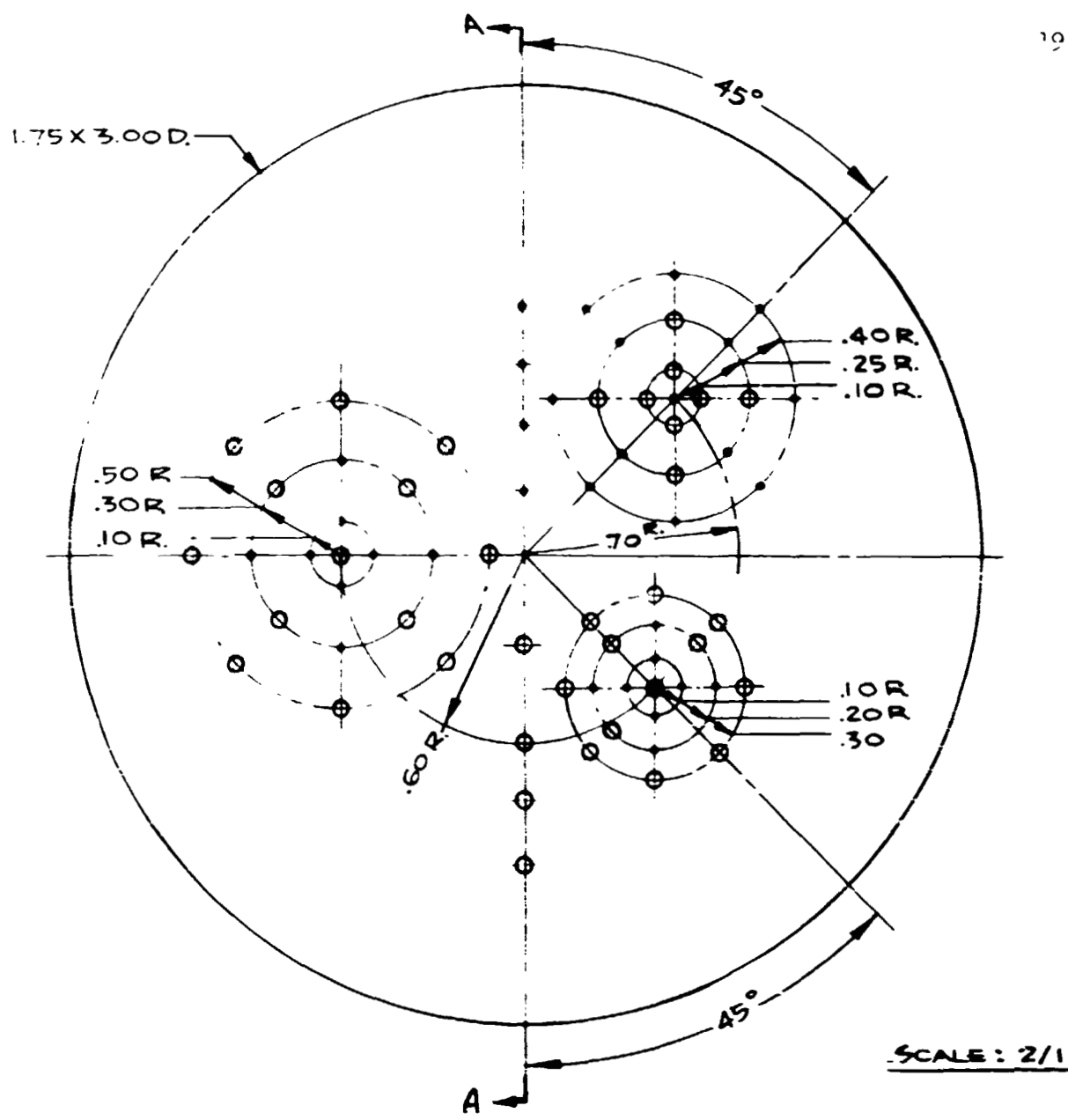


Figure 8 - Typical Time History of Surface Temperature (240 Second Test Shown)
Material - Phenolic Nylon W/Microballoons



HOLE SYMBOL	HOLE DIAMETER	HOLE DEPTH CLUSTERS	LINE AT A-A	COPPER WIRE BACKING
O	.0700	0.70 IN.	25 INCREMENTS OUTBOARD RADIALY TO	*12- .081 DIA.
•	.0465	0.70 IN.	1.00 TOTAL DEPTH	*14- .064 DIA.

Figure 9 - Insert Arrangement (Random Hole Patterns)
200-Second Test Specimen

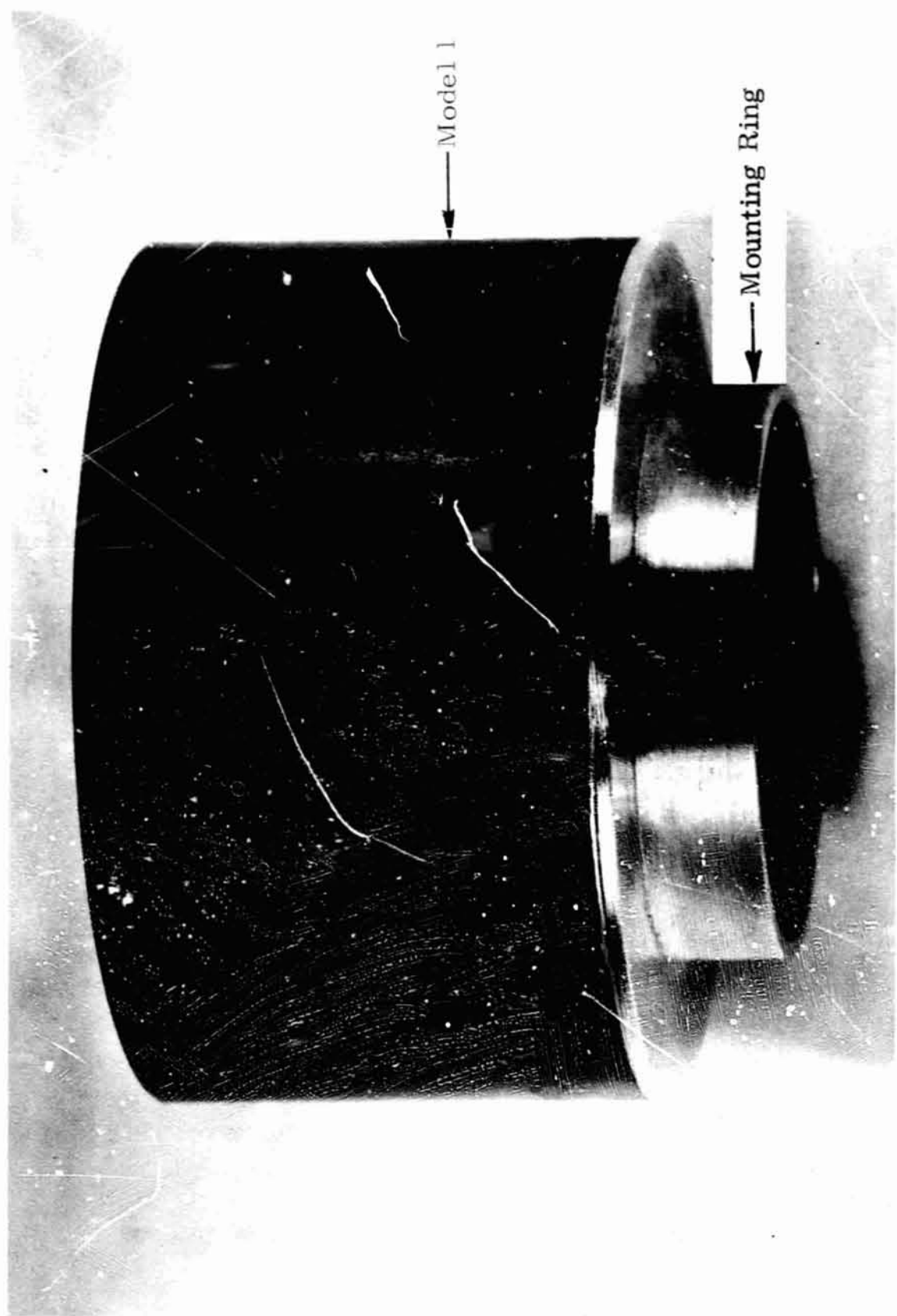


Figure 10 - Profile Photograph of 200-Second Specimen
(Before Test)

Model 1

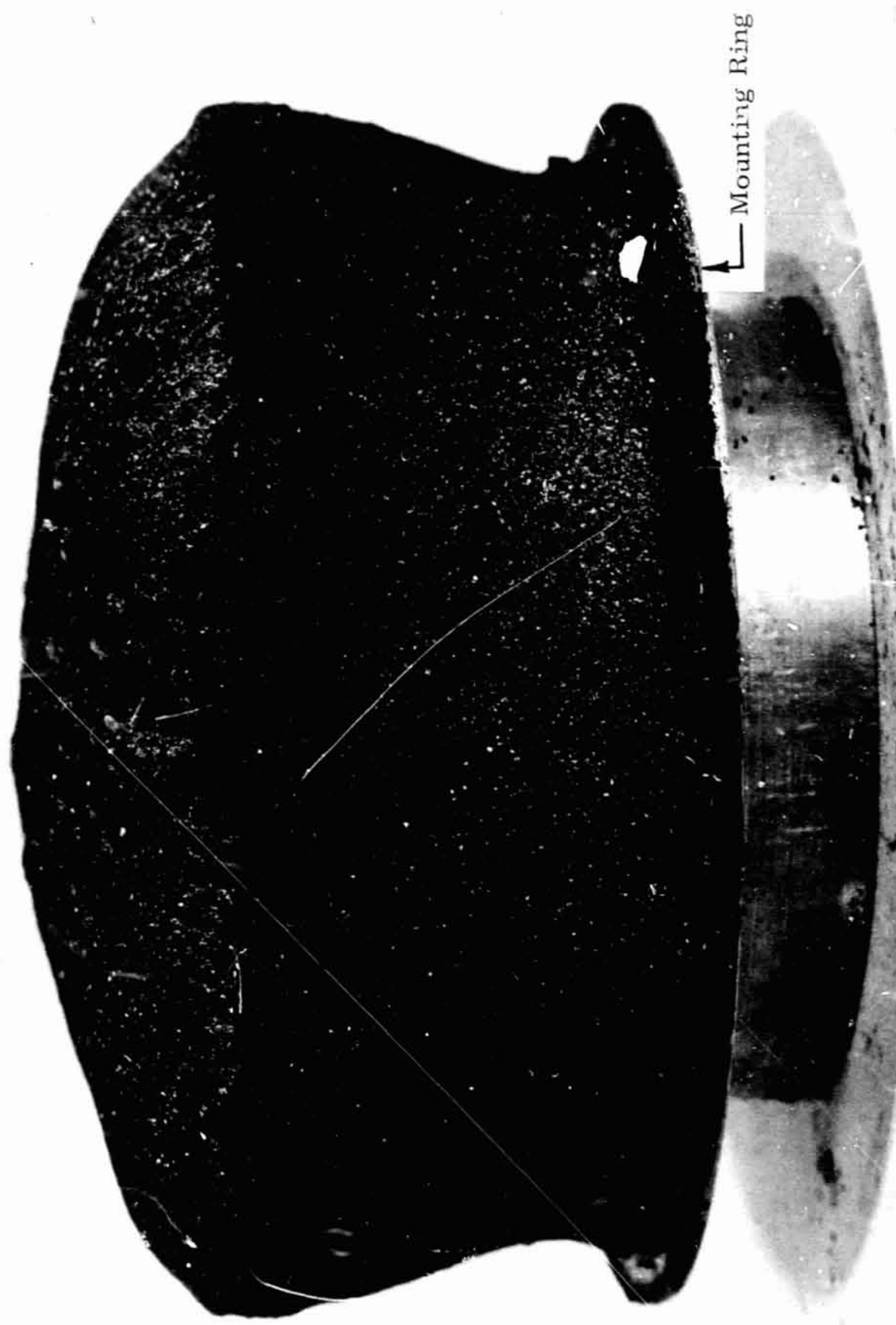
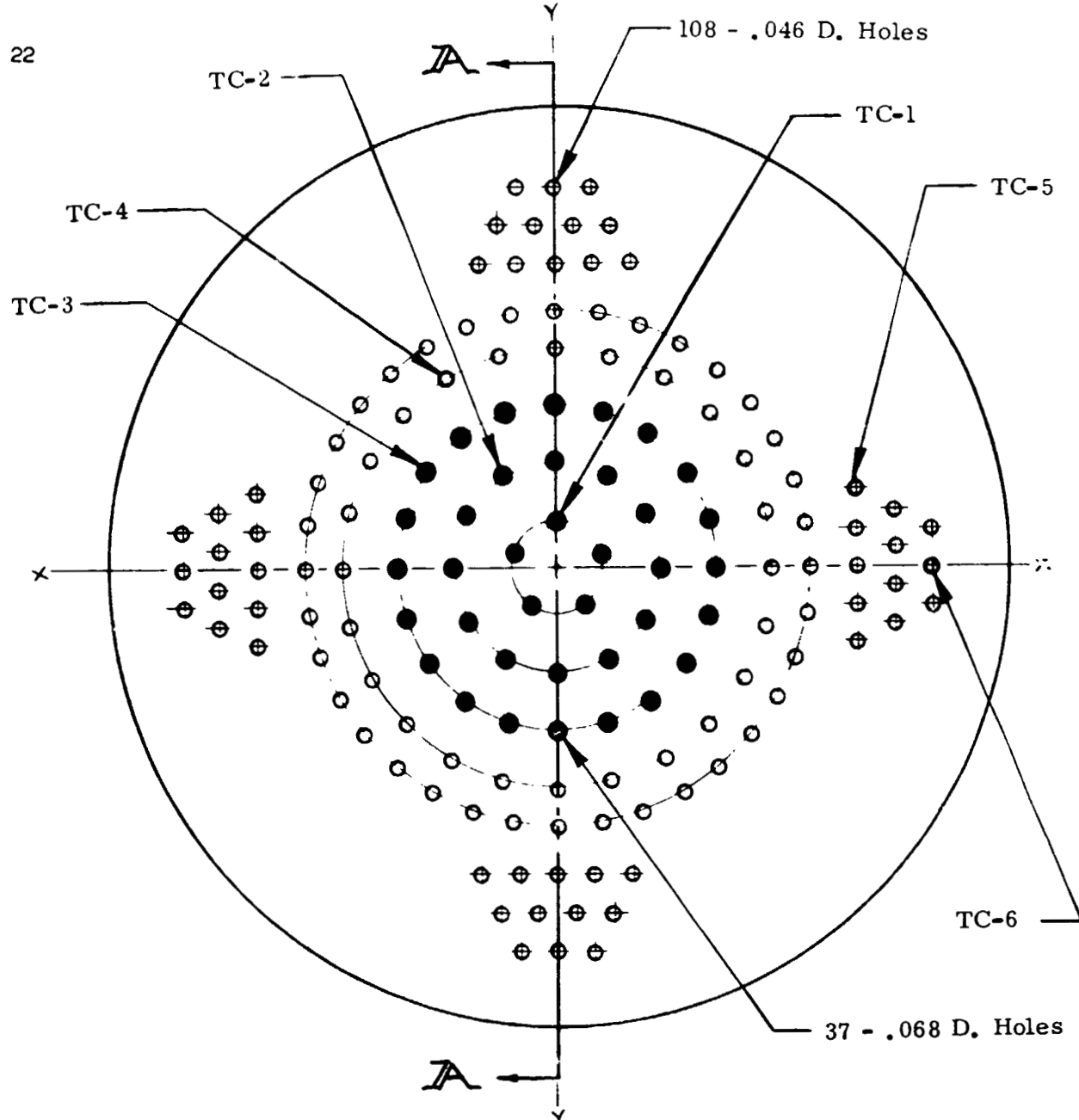


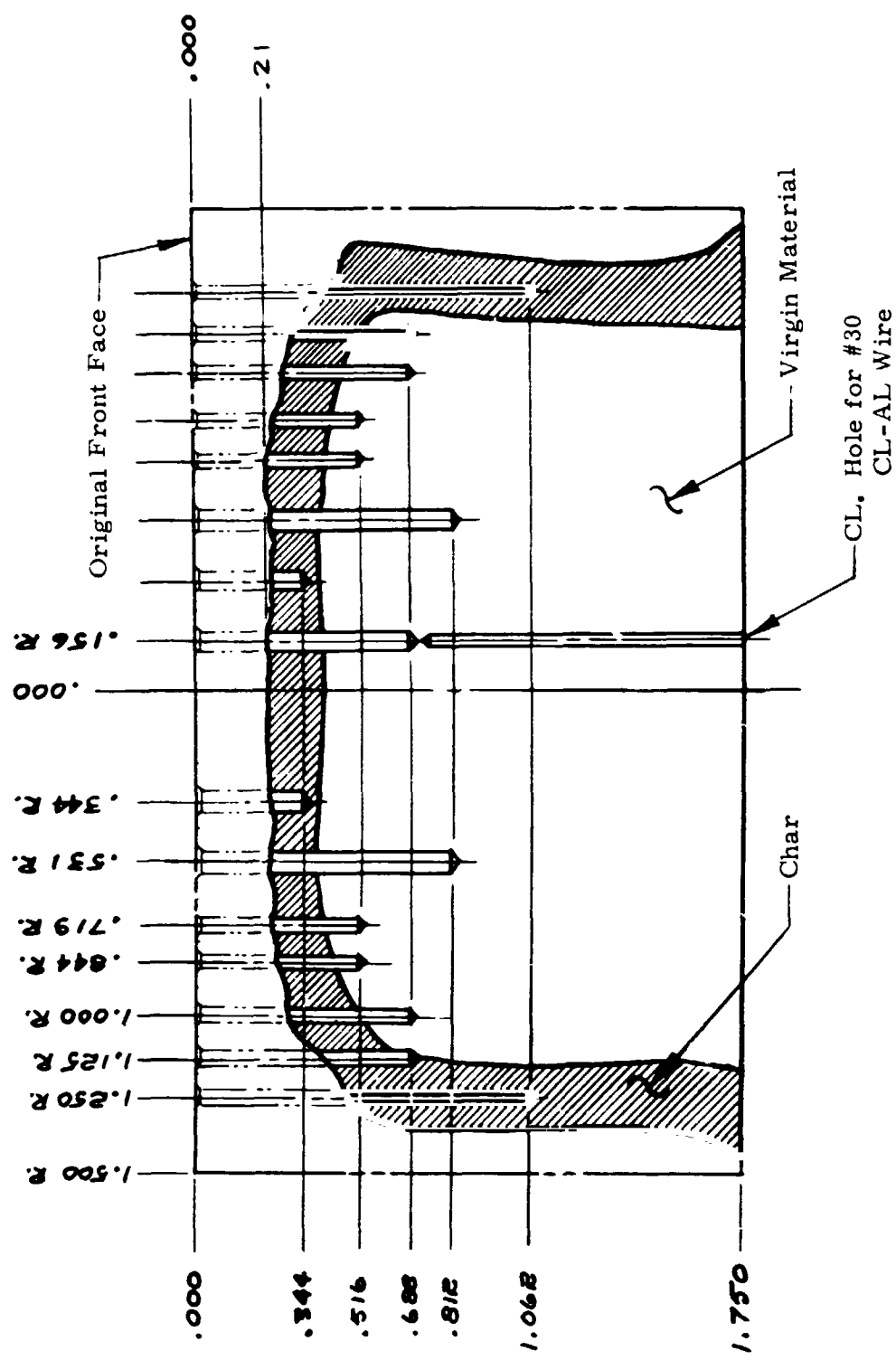
Figure 11 - Profile View Showing Appearance After 200-Second Test



• LEGEND •

- - No. 16 Pin Hole (For No. 16 and 14 Ga. Wire Leads)
- - No. 20 Pin Hole (For No. 18, 20, and 22 Ga. Wire Leads)
- TC - Thermocouple Locations

Figure 12 - Insert Arrangement - 160- and 80-Second Test Specimen



23

Figure 13 - Contour and Hole Depth Measurements
(80-Second Test)

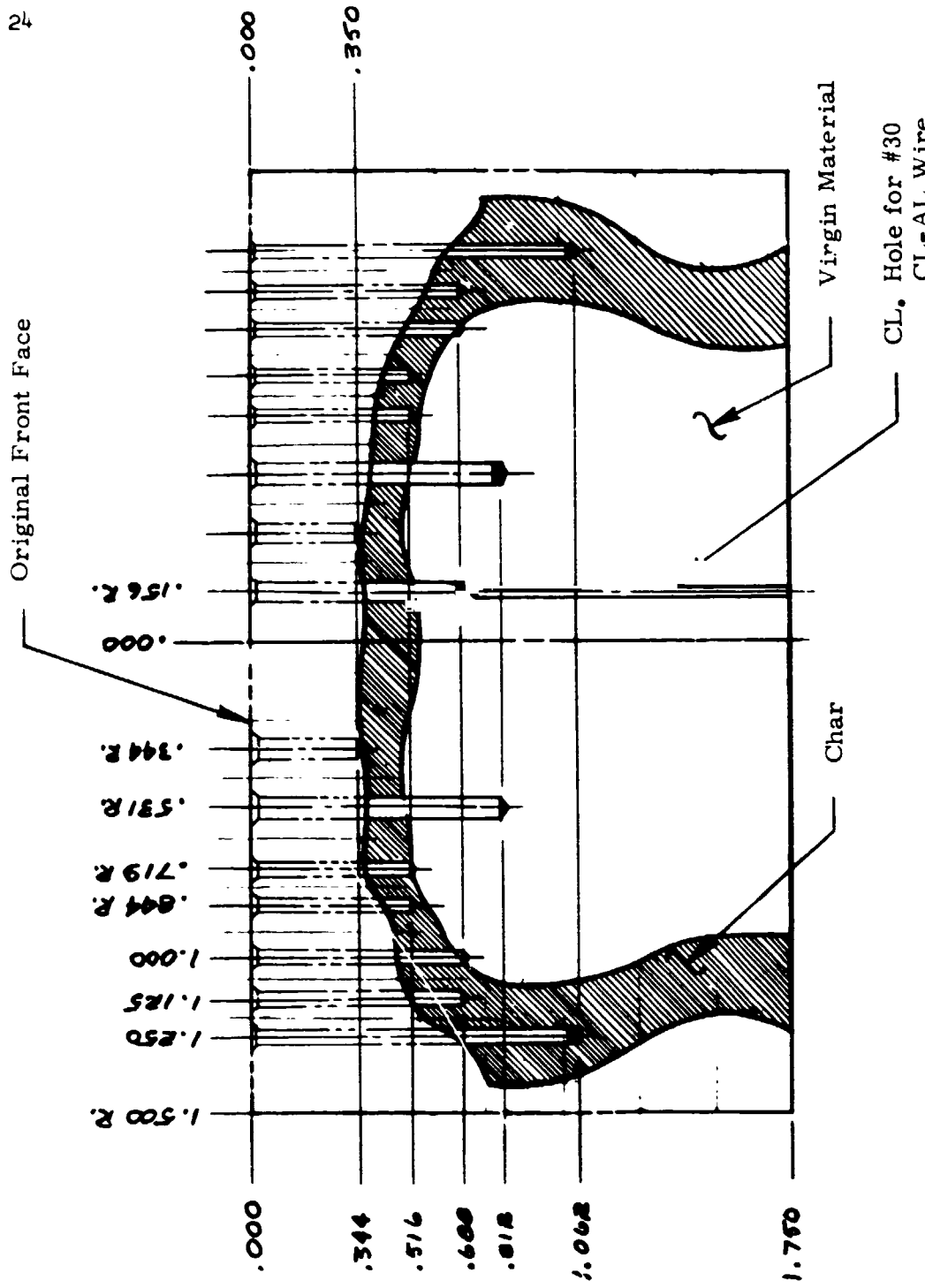


Figure 14 - Contour and Hole Depth Measurements
(160-St. 1nd Test)

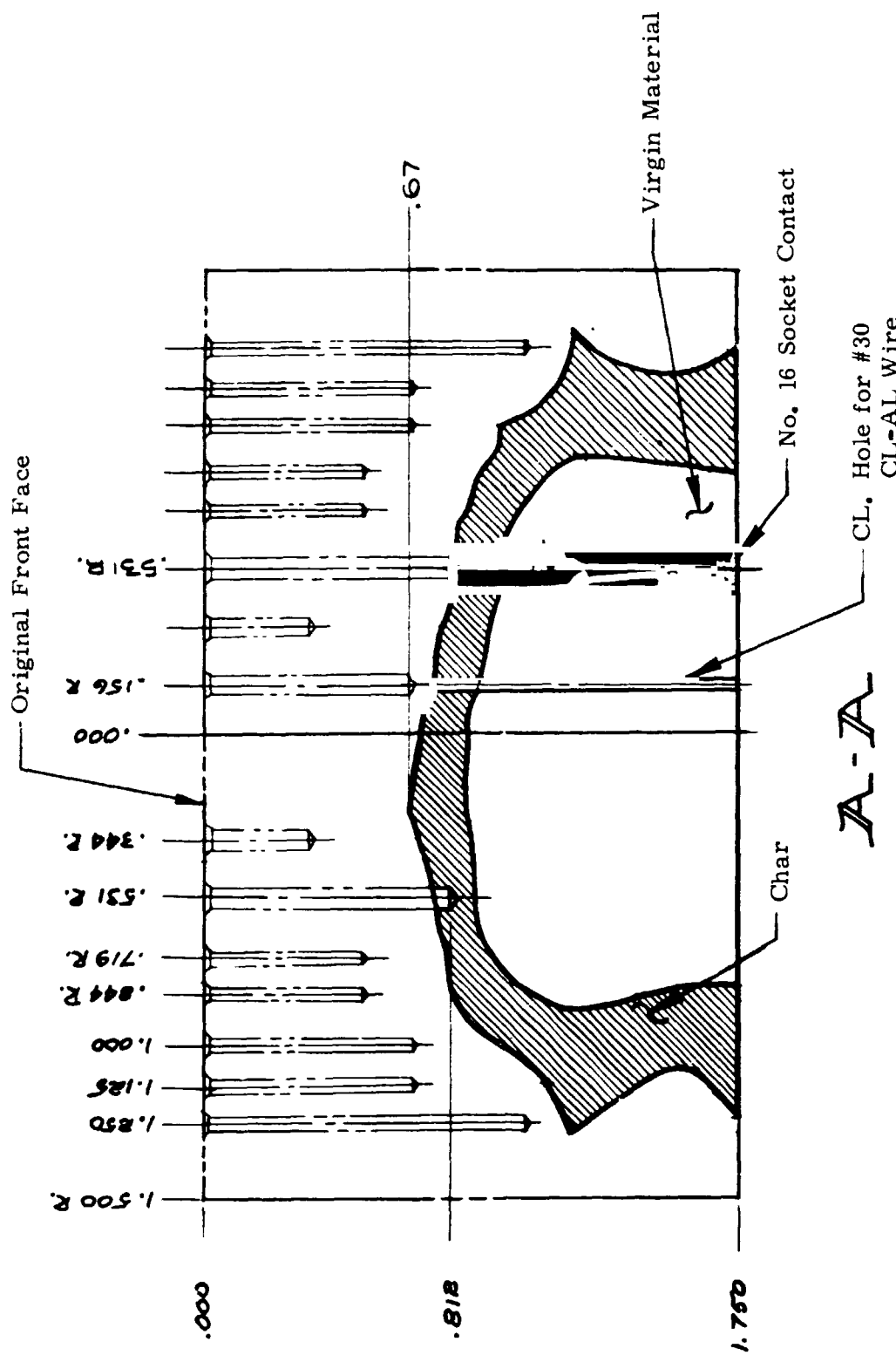


Figure 15 - Contour and Hole Depth Measurements
(240-Second Test)

Phenolic Nylon W/Microballoons
 $q = 110 \text{ BTU/ft}^2 \text{-sec.}$

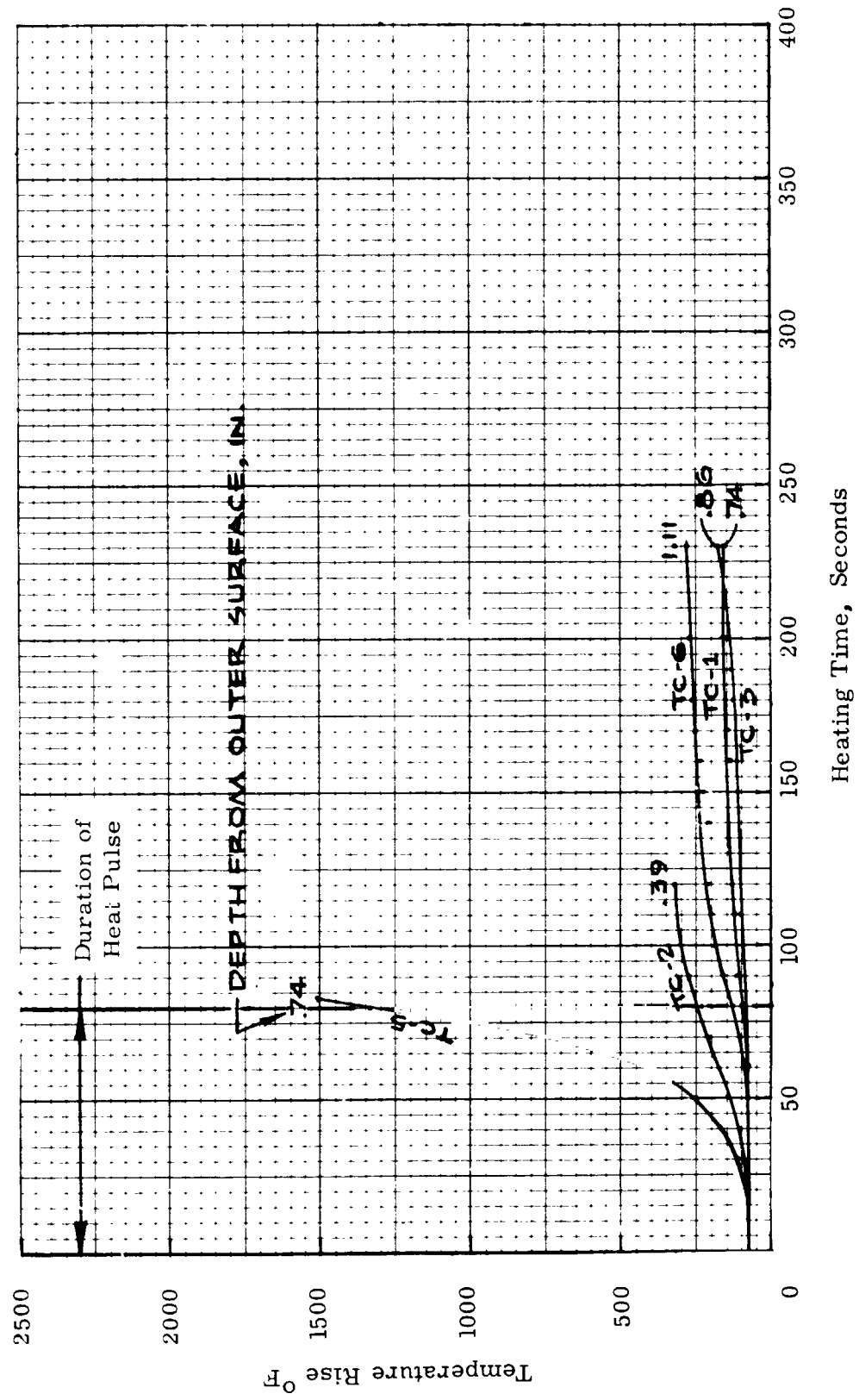
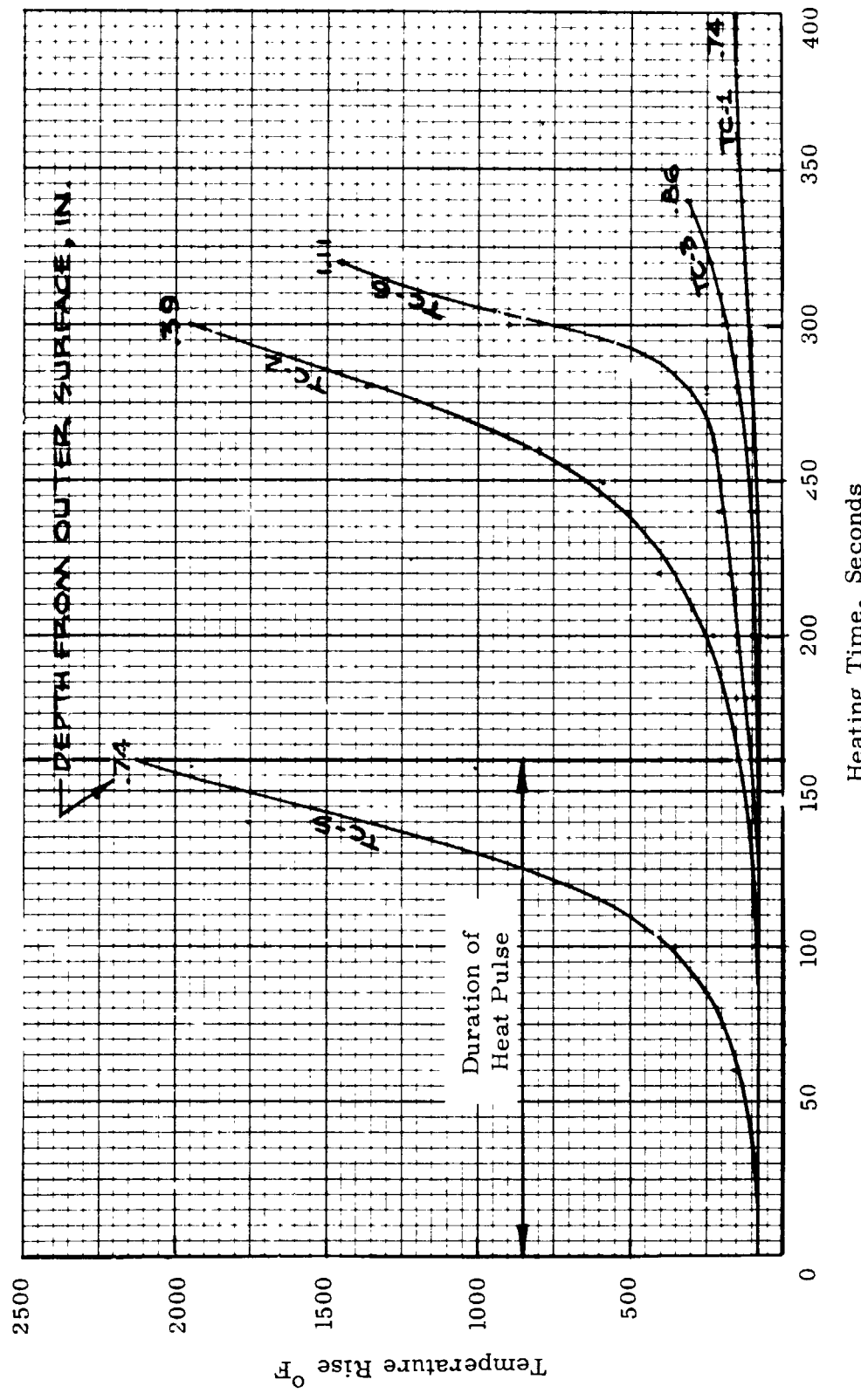


Figure 16 - Temperature - Time History
 (Test Exposure Time - 80-Second)

Phenolic Nylon W/Microballoons
 $q = 110 \text{ BTU/ft}^2 \cdot \text{sec.}$



27

Figure 17 - Temperature - Time History
(Test Exposure Time - 160-Second)

PHENOLIC NYLON W/MICROBALLOONS

$$q = 110 \text{ BTU/FT}^2 \text{-sec.}$$

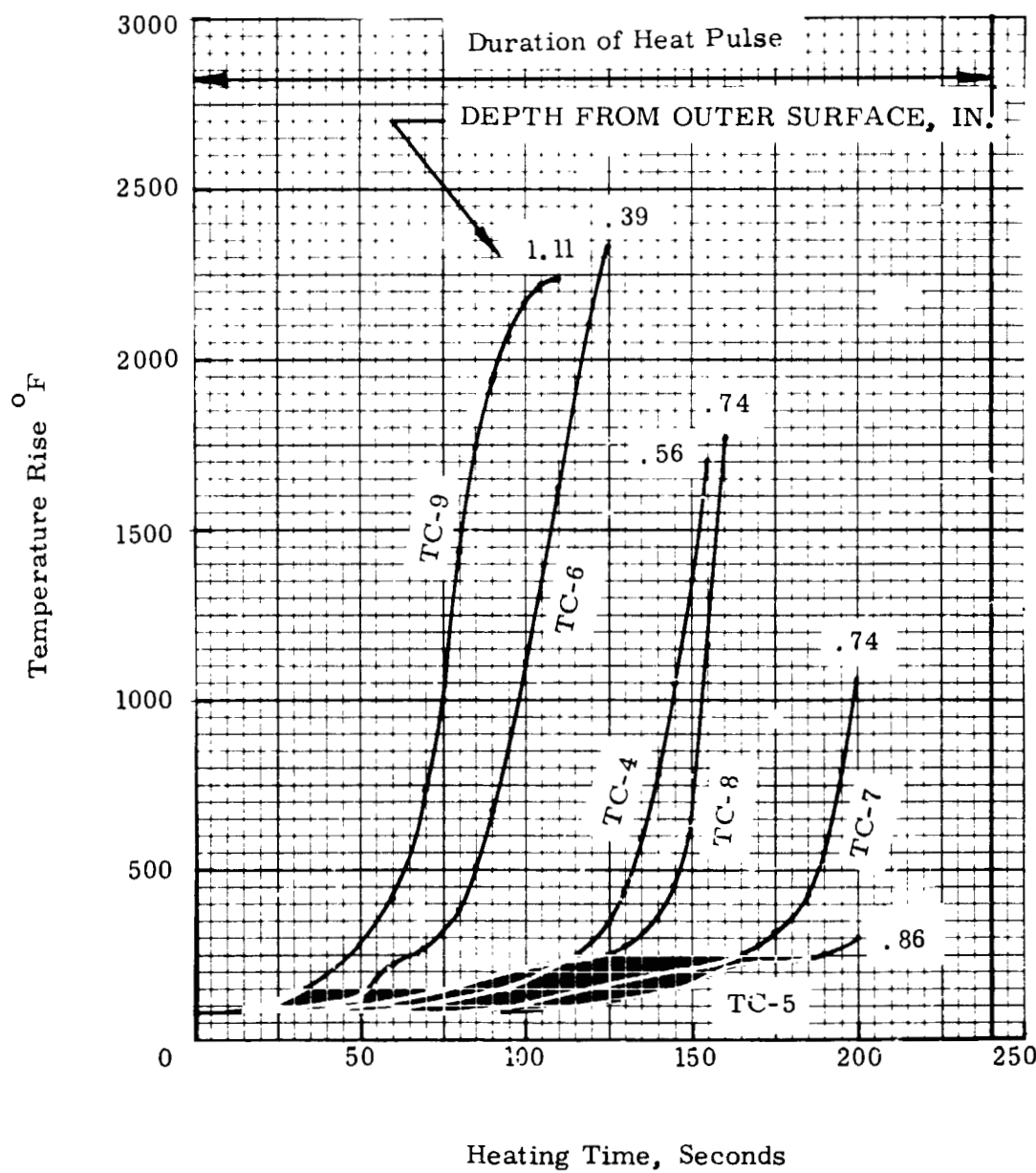


Figure 18 - Temperature - Time History
(Test Exposure Time - 240-Second)

Phenolic Nylon W/ Microballoons
 $q = 110 \text{ BTU}/\text{ft}^2 \cdot \text{sec.}$

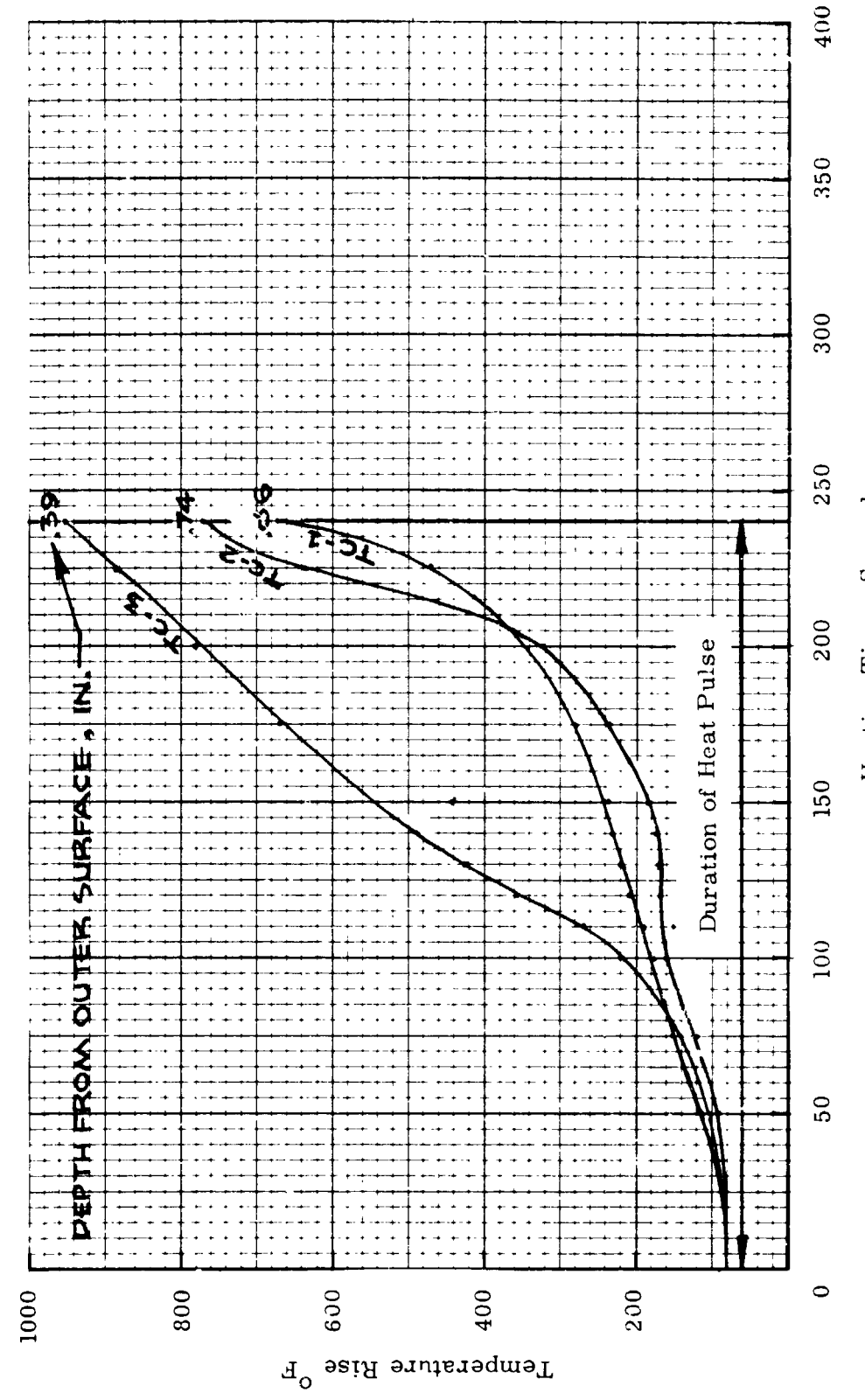


Figure 19 - Temperature - Time History for Socket Contacts
(Test Exposure Time - 240-Second)

PHENOLIC NYLON W/ MICROBALLOONS

$$q = 110 \text{ BTU/FT}^2\text{-sec.}$$

30

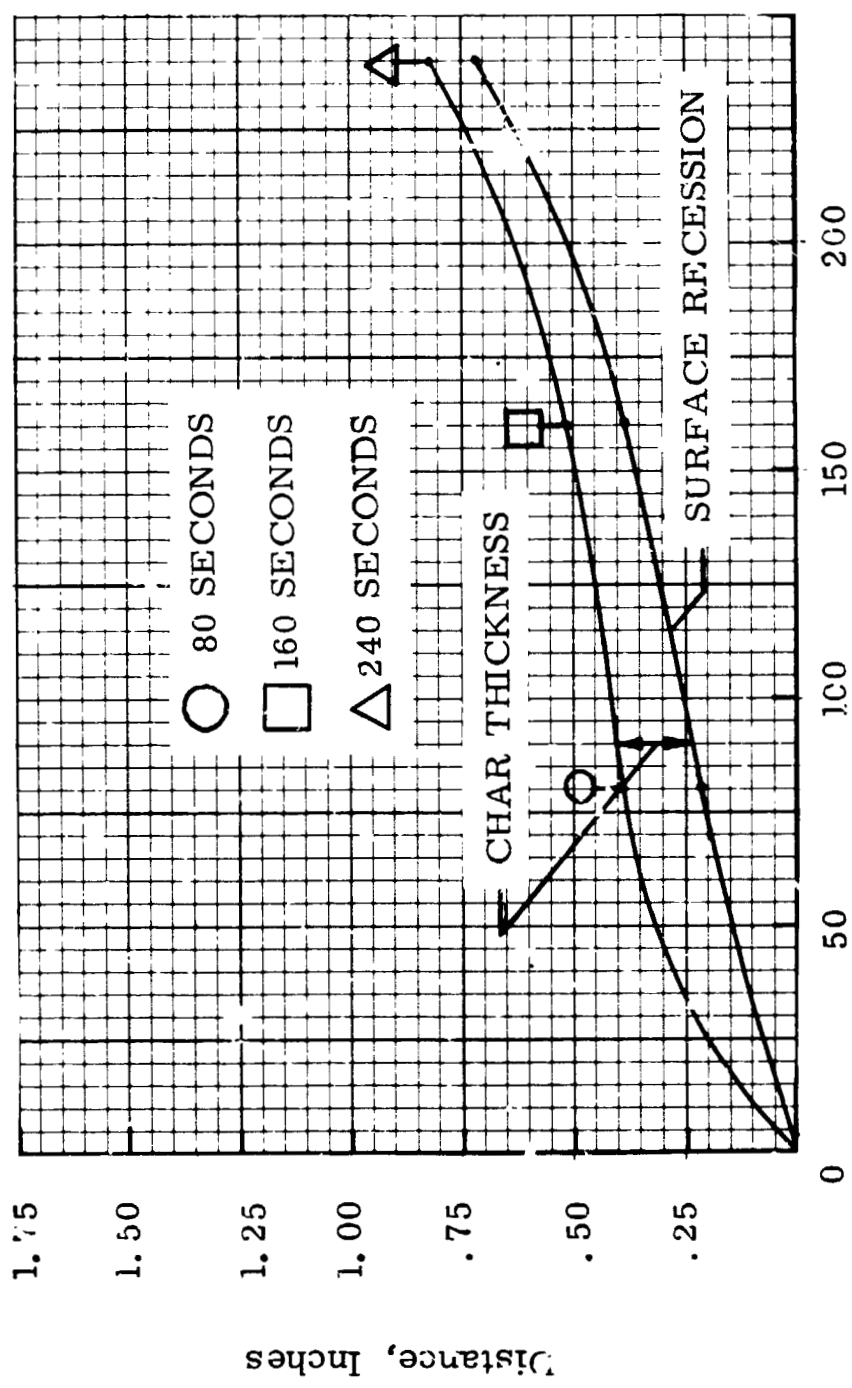


Figure 20 - Time History of Surface Recession and Char Growth

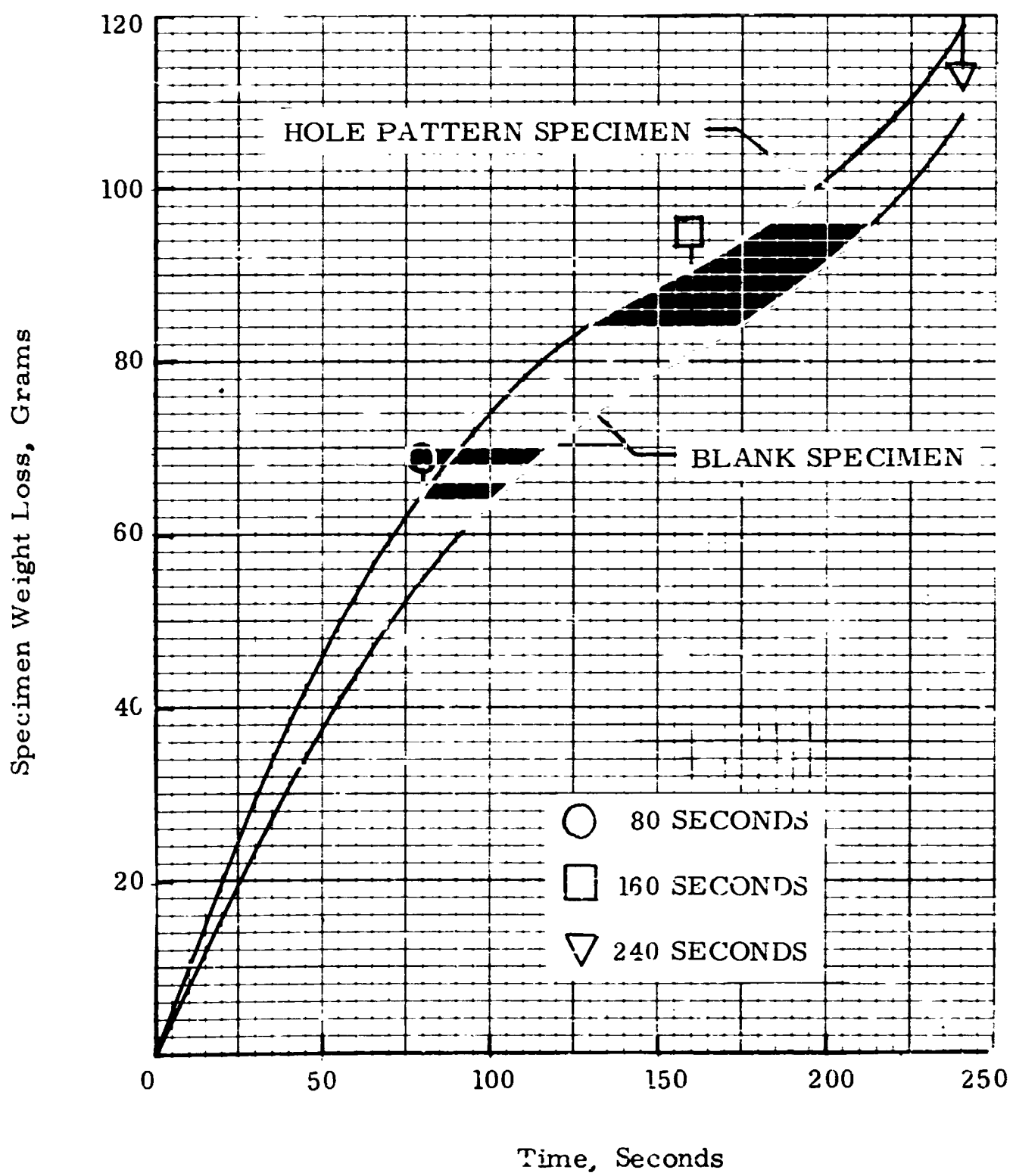
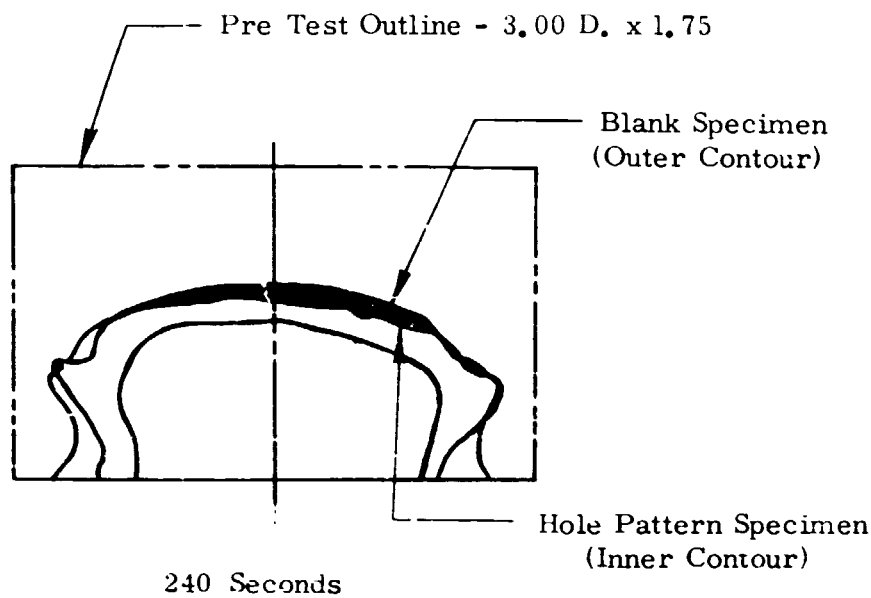


Figure 21 - Comparison of Weight Loss

32



Note: Blank specimen has smooth contour characteristic, contrary to hole pattern specimen where holes are in a cratered condition as noted in detail "a".



Detail "a"
Scale: 2/1

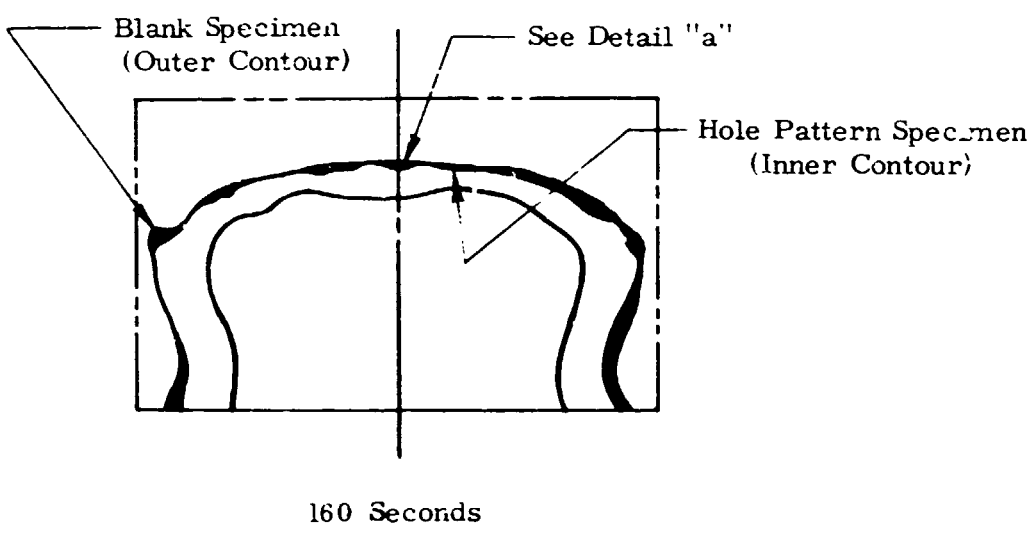


Figure 22 - Comparative Ablation of Phenolic-Nylon
W/ Microballoons Specimen

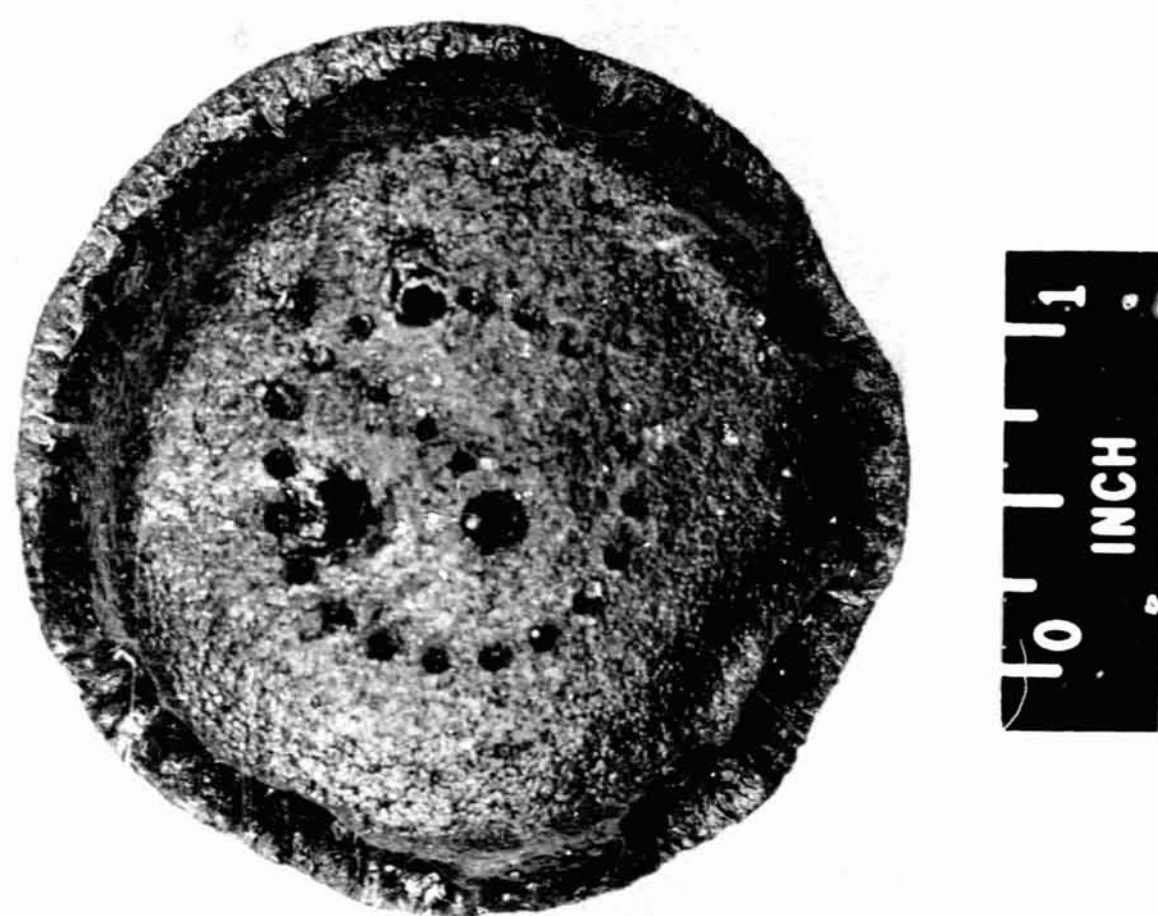


Figure 23 - Top View of Model 2 Showing Effect of 240-Second Exposure to the Test Environment



10 1
INCH

Figure 24 - Profile View of Model 3 Showing Effect of 240-Second Exposure to the Test Environment

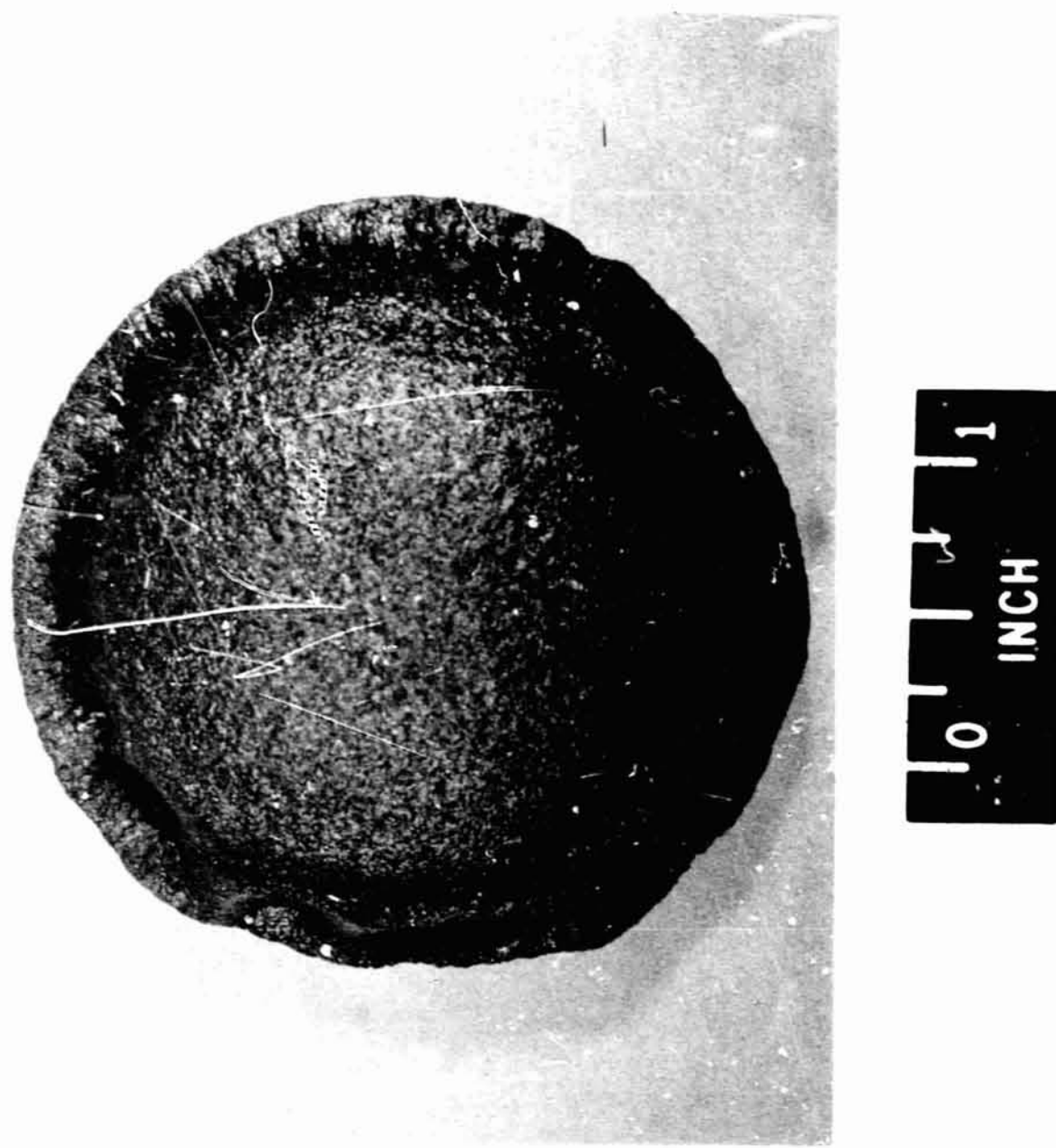


Figure 25 - Top View of Model 4 Showing Effect of 160-Second Exposure to the Test Environment

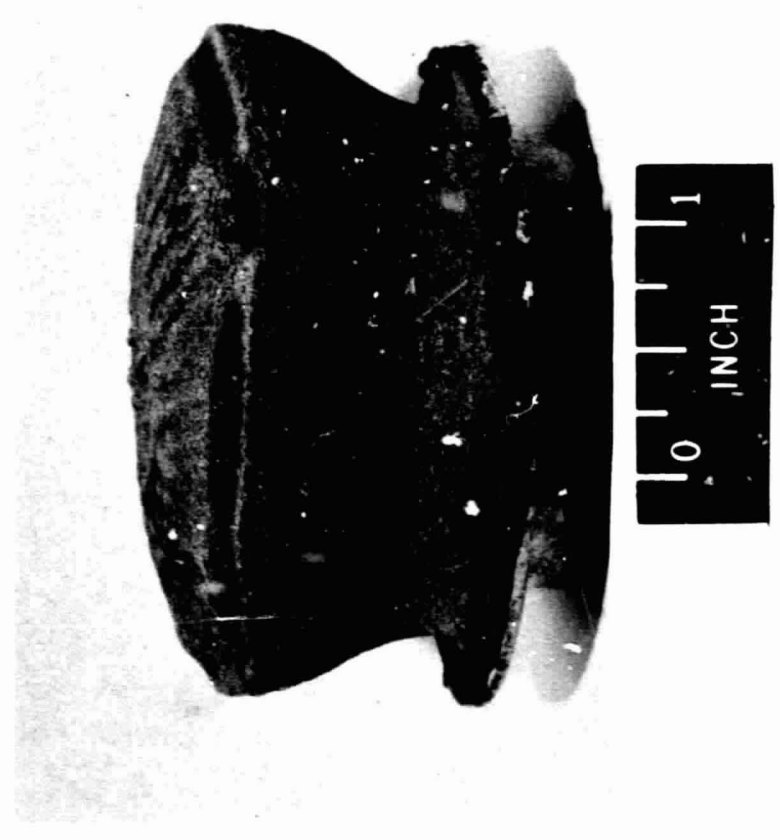


Figure 26 - Profile View of Model 4 Showing Effect of
160-Second Exposure to the Test Jet
Environment

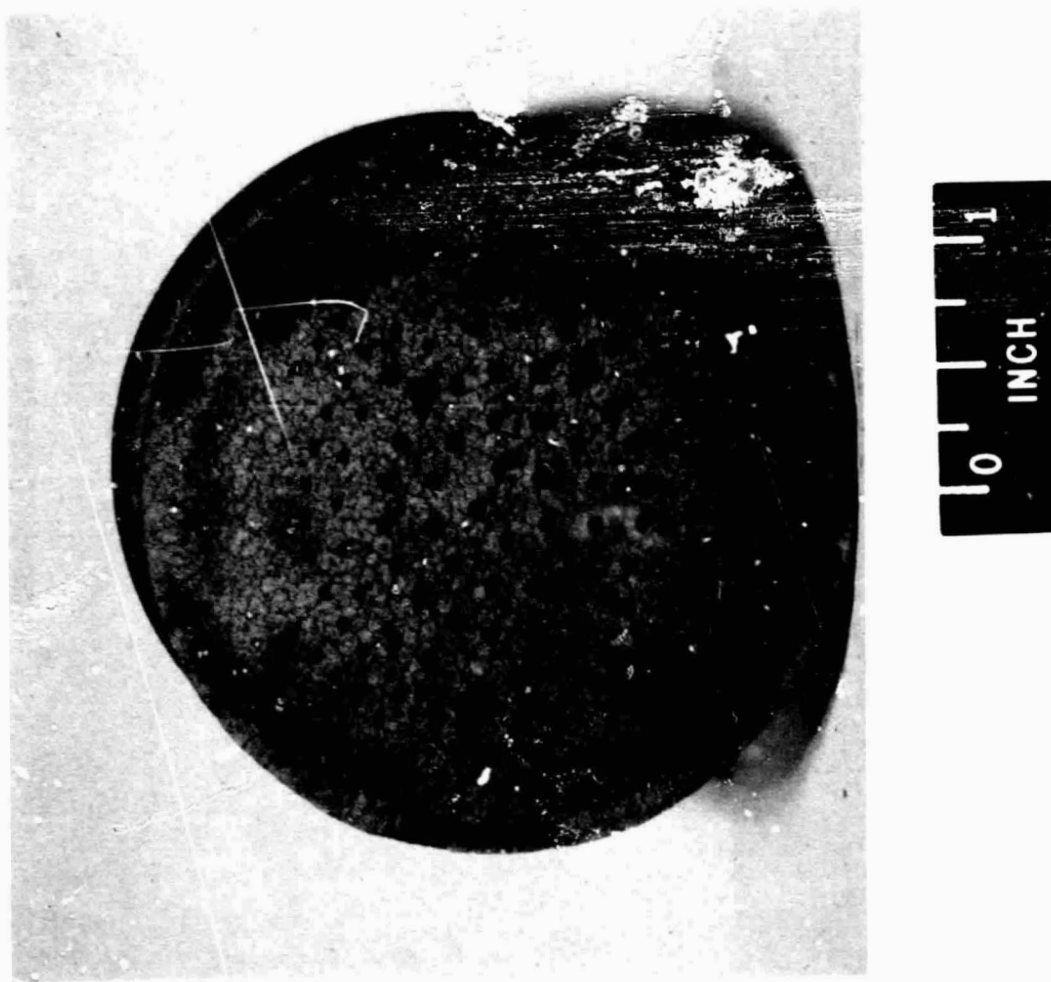


Figure 27 - Top View of Model 6 After 80 Seconds
Exposure to the Test Environment

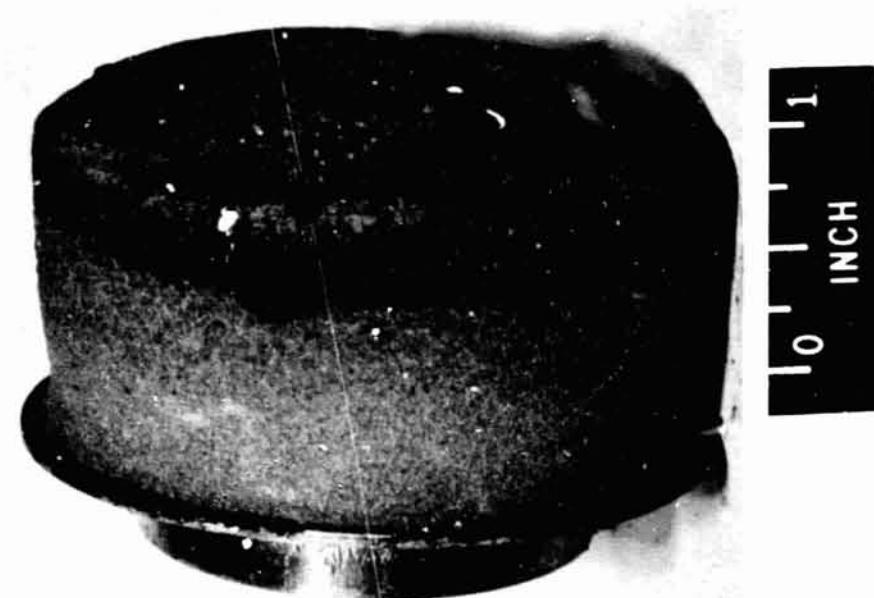


Figure 28 - Profile View of Model 6 After 80 Seconds
Exposure to the Test Environment